Response to Referee #1

Thank you very much for reviewing our manuscript and providing potential comments.

General Comment: This study presents an analysis of 3-hourly radiosonde data taken over 3-day intervals in each month over several years. The focus is on identifying the boundary layer height. This height is divided into convective and stable boundary layers and also residual layers. Several methods are used to identify the top of the ABL, but they are all based on gradients. These methods are appropriate, and the comparison of the methods is a nice aspect of this study. The diurnal cycle of ABL height is described; the upshot seems to be that there is a strong diurnal cycle but the amplitude is affected by the season as well as the presence of clouds, which also appear to affect the phase. Overall, the presentation of the results is clear, but the weakness is that it is not clear whether the results provide novel insight. Instead, the novelty appears to be in the data set itself. There are several areas where some additional work could improve the analysis. These are relatively minor issues. The text is written well, but could stand another round of close editing for small grammatical and English issues (some examples listed below).

Reply: We have taken all the suggestions and incorporated into the revised manuscript.

Comment 1: Perhaps the main issue I have with this study is that it is quite focused on the radiosondes, with limited support from other observations. This becomes crucial as the text explores the impact of clouds on the ABL structure. There is a good use of IR brightness temperature to provide an estimate of cloud top height, but this is the only cloud observations that are presented. I found that to be surprising. Perhaps even more surprising once I visited the NARL website (https://www.narl.gov.in/) and found that there are several instruments that could provide useful supplementary data. One that could provide highly complementary data is the microwave radiometer; the web site says that it retrieves cloud base and liquid water path. These could be quite useful for more clearly defining the cloud layer. There are also radiation sensors and eddy covariance latent and sensible heat fluxes that could be used to construct a surface energy balance. There are also rain gauges and a disdrometer, which could be used to explore the ABL height as a function of rain rate. Such an analysis could bolster the conclusions about deep convection having little impact on the ABL height.

Reply 1: Certainly appreciate the reviewer's suggestion to utilize the microwave radiometer data for the cloud layer information and boundary layer tower data to calculate the surface energy balance. Unfortunately, these datasets is not available during observation periods used in this study. Reviewer 2 also pointed to obtain the cloud layer using relative humidity (RH) data (See response to reviewer#2). We have checked the rainfall data obtained from rain gauges (Automatic weather station data), but we could not find any relation between the ABL and rainfall.

Changes in the manuscript 1:
(~Line 146-148) Most of the observations are conducted during non-rainy days except two during 01:00 IST-02:00 IST on 18 August 2011 and 14:00 IST-20:00 IST on 21 August 2012, with total rainfall about 47 mm and 46 mm, respectively.

(~Line 630) It is to be noted that there are two occasions when rainfall occurred during the campaign periods, however, these few data do not reveal any relation between the ABL and rainfall.

Comment 2: The histograms of Figure 7 raise an issue about the statistics being used. Most of the histograms (which are NOT pdfs) look very non-Gaussian. The text mentions that the peak of the SBL histogram is at a substantially lower altitude than the mean (also true for RL in summer). Based on these histograms, I suggest also reporting the median and interquartile range, which provide a better estimate of the typical values and variability of the data.

Reply 2: The distribution shown in Fig. 7 is non-Guassian especially for the SBL distribution which has longer tail on the right and hence positively skewed. As suggested, we have also included the boxplot of

the SBL, CBL and RL heights for the annual, winter and summer monsoon as shown in Fig. 8 in the revised manuscript.

Changes in the manuscript 2:
(~Line 468-475) We also obtained the distribution of the SBL, CBL and RL for the annual, winter and summer monsoon in terms of the boxplot as shown in the Figs. 8a-c, respectively. The median values the SBL during the annual, winter and summer remain same (Fig. 8a). There are a few outliers whose values are greater than 3 times of the corresponding interquartile ranges (IQR) for the annual and two different seasons. The SBL mostly lies below 0.65 km during the winter and 0.4 km during summer monsoon. The SBL is more variable during the winter than summer monsoon. As mentioned earlier, the CBL is higher and more variable during the summer monsoon than winter (Fig. 8b). Similarly, the RL is also more variable during the summer monsoon than winter (Fig. 8c). In contrast to the CBL, RL is lower during the summer monsoon when compared to winter.

Comment 3: I found the definition of the residual layer (RL) to be a little unclear. It seems to be defined exactly the same as for the CBL, is that correct? It would be good to include an explanation in Section 2.3.

Reply 3: The method to obtain the RL is similar to that of the CBL. As the RL is the part of the daytime ABL, its characteristic is entirely similar to that of CBL except RL does not connected to surface whenever SBL is present. However, for the case when the SBL is absent RL is connect to the surface and generally referred as neutral RL (NRL) (Liu and Liang, 2010). However, we have referred it as simply RL. This aspect has been mentioned in the manuscript.
Liu, S. and Liang, X.-Z.: Observed diurnal cycle climatology of planetary boundary layer height, J. Climate, 23, 5790-5809, 2010.

Changes in the manuscript 3:
(**~Line 193**) The method to obtain the RL is similar to that of the CBL.

Comment 4: One aspect of the residual layer that has been pointed out as being important for the diurnal evolution of the ABL is that it provides the potential for "explosive growth" of the ABL as a CBL forms in the morning and grows into the RL. This was not mentioned in this paper. Is it possible to quantify whether this explosive growth occurs, or are the 3-hourly observations too infrequent?

Reply 4: This is a good point. We have included this information in the revised manuscript. One can simply obtain the difference between ABL height before and after the sunrise, in order quantify the CBL growth. However, from typical diurnal variations (See Fig. 4), it can be seen that the transition from RL to CBL is not always explosive.

Changes in the manuscript 4:
(~Line 60-62) One aspect of the RL that has been pointed out as being important for the diurnal evolution of the ABL is that it provides the potential for "explosive growth" of the ABL as a CBL forms in the morning and grows into the RL.

Comment 5: The correlation analysis among the ABL height definitions is quite nice. I was surprised there was not a similar correlation analysis between the surface temperature and the ABL height (around lines 427-455). In particular with regard to the seasonal variation that is mentioned, it would be nice to see whether the ABL height is related to the, say, the absolute maximum temperature or the diurnal temperature range.

Reply 5: We have obtained the scatter plot of the surface temperature and ABL height. The scatter diagrams of the surface temperature and the different ABL regimes such as the CBL, RL and SBL indicate that their relations are random in nature. Though CBL and RL become higher with higher surface temperature and vice versa, there are several occasions when they vary randomly.

Changes in the manuscript 5:
(~Line 547-553) As mentioned earlier, the diurnal evolution of the annual and seasonal mean pattern of the ABL is closely associated with the surface temperature. In order to see their 3-hourly relationships, we obtained the scatter plot of the CBL, RL and SBL with the surface temperature as shown in Figs. 11a-c, respectively. Broadly, the scatter diagram indicates that warmer is the surface, the higher is the CBL and RL and vice versa (Figs. 11a-b). However, these features are not always consistent and several times they occur randomly. In contrast to the CBL and RL, SBL higher is higher over the colder surface and vice versa, however, these features also are not always consistent and several times they occur randomly (Fig. 11c).

Comment 6: Several places in the text seem to indicate that the presence of clouds might alter the evening transition (ET). This was never made completely clear. Is there a relationship or not? If there is, can it be understood in terms of the longwave effect that is mentioned, or is the mechanism unclear?

Reply 6: The presence of the cloud could be one possible reason to alter the evening transition. However, there are occasions when the SBL forms even in the presence of the clouds (See Table 1). So at this juncture, it is not possible to provide a clear mechanism only based on the cloud information.

Changes in the manuscript 6:
(~Line 355-358) However, it must be noted that presence of the clouds could be one possible reason as there as occasions when the SBL forms even in the presence of the clouds. Hence, the delay in the ET process cannot be entirely explained by the longwave effect.

Technical Comments

Line 32: Start the sentence with "The"
Reply: Corrected.

Line 36: change to "balance between the surface"
Reply: Changed.

Line 37-38: change to "The ABL height is a key parameter, providing a length scale for..."
Reply: Changed.

Line 51: insert a dash ("–") between maintenance and rather
Reply: Inserted.

Line 54: delete the extra "m"
Reply: Changed.

Line 66: I think there are many more studies of the diurnal variation of ABL height than this sentence would lead the reader to believe. There are recent examples using ARM sites (Santanello et al, 2007, http://dx.doi.org/10.1175/JHM614.1; May et al., 2012, http://dx.doi.org/10.1175/JCLI-D-11-00538.1), but there are also older examples from field studies (Brill & Albrecht, 1982, http://dx.doi.org/10.1175/1520-0493(1982)110<0601:DVOTTW>2.0.CO;2) or observation sites (Hashiguchi et al., 1995a, Boundary-LayerMeteorology 74: 419-424; Hashiguchi et al., 1995b, http://dx.doi.org/10.1029/95RS00653), and even in more exotic settings (e.g., on a glacier, van den Broeke, 1997, Boundary-Layer Meteorology 83: 183–205).
Reply: We thank for updating these references which are cited in the revised manuscript.

Changes in the manuscript:
(~Line 86-104) There are several case studies focusing on the diurnal structure of the boundary layer and the mechanism responsible for its formation over different regions of the globe. Brill and Albrecht, (1982) presented the diurnal variation of the cloud fraction and trade-wind inversion base height using the data collected from various ships and aircraft. May et al., (2012) have studied the diurnal variation of convection, cloud, radiation, and boundary layer structure in the coastal monsoon environment (Darwin, Australia). Santanello et al., (2007) has studied the feedback of soil moisture dryness on the development of the convective boundary layer over the southern Atmospheric Research Measurement Program–Great Plains Cloud and Radiation Testbed (ARM-CART) sites. During a clear sky day Hashiguchi et al., (1995a) observed boundary layer radar echo indicating the ABL height. Hashiguchi et al., (1995b) further observed that the boundary layer radar detects diurnal variation of the ABL both at the equatorial and midlatitude regions. During the summer over a midlatitude glacier, the diurnal and vertical and horizontal structures of the boundary layer were found to be dominated by persistent glacier winds forced by gravity (Van den Broeke, 1997).

Line 72: Also see Seidel et al. (2012, http://dx.doi.org/10.1029/2012JD018143).
Reply: Cited.

Line 90: change to "... days in each month..."
Reply: Changed.

Line 100: delete "continuously"
Reply: Deleted.

Line 106: delete "at"
Reply: Deleted.

Line 184: delete "convective"
Reply: Deleted.

Line 192: insert "as" before easy
Reply: Inserted.

Line 231: change "is" to "are"
Reply: Changed.

Line 239: Doesn't this ABL structure seem similar to a shallow cumulus profile, or a decoupled cloud-topped ABL, as is often described over the ocean in the transition from stratocumulus to cumulus?
Reply: Yes, it seems like a shallow layer cloud decoupled from the surface. The surface moisture is very small and the LCL is observed at about 0.6 km and CTH is at about 0.81 km indicating that a shallow layer cloud of thickness about 0.2 km decoupled from the surface.

Changes in the manuscript:
(~Line 291-293) The surface moisture is very small and the LCL observed at about 0.6 km which indicates that a shallow layer cloud of thickness about 0.2 km decoupled from the surface (Garratt, 1992).

Line 291-292: change to "... ET process was not delayed and ..."
Reply: Changed.

Line 292: I think this should read "On the third night the SBL was detected at a height near 0.45 km."
Reply: Modified as suggested.

Line 298: Delete "till"
Reply: Deleted.

Figure 6b: This bar chart is difficult to read, the format in Figure 9 is much better.
Reply: Figure 6b is modified as Figure 9.

Response to Referee #2

Thank you very much for reviewing our manuscript and providing potential comments.

General comment: The authors have used data collected by the radiosondes over a tropical station and deduced the boundary layer height. The data were collected over 3-year period during various field campaigns. They have shown the diurnal, and seasonal cycle of boundary layer depth. Further they have classified the boundary layer structure into different categories like convective, stable and residual and have reported the statistics of those as well. The authors have made a good attempt to report the statistics but they fall short in deriving any scientific conclusions from them, leaving the reader with a feeling that no manuscript is simply a collection of statistics. I suggest the manuscript to go through a thorough revision before being published. Below I have listed my major and minor concerns.

Reply: We have taken all these suggestions and incorporated into the revised manuscript.

Major Concerns:

Comment1) As I mentioned earlier, the paper seems like a collection of statistics. You have mentioned in the abstract that various studies have reported the boundary layer depth from that station. So I am not sure of the purpose of this paper is to validate them, or to report them again or to gain some scientific insights on the causes of the changes in the boundary layer depth. It will be good if you can clarify it in the introduction section.

Reply 1: There have been several case studies over the station, but none of them has classified the ABL into different regimes such as CBL, SBL and RL and has not been dealt separately during different seasons. The effect of the cloud on the diurnal structure of the ABL is also, has not been attempted yet before this study.

Changes in manuscript 1

(~ Line 122-125) Making use of this dataset (radiosonde data), first time complete diurnal variability of the ABL height and their classification into different ABL regimes such as the CBL, SBL and RL during different seasons and effect of the cloud in its diurnal structure has been studied and the results are presented in this paper.

Comment 2) As you have radiosonde data, I suggest you calculate the lifting condensation level (LCL) and also report its variation for the different boundary layers. Please refer to Bolton (1980) regarding the calculations. Add the LCL to Figure 8 and 10.

Reply 2: We have added the lifting condensation level (LCL) in the revised manuscript.

Changes in manuscript 2:

(~Line 203-211) The lifting condensation level (LCL) is defined as the height at which an unsaturated air parcel becomes saturated (RH >100%) when it is cooled by dry adiabatic lifting (Wallace and Hobbs, 2006). It provides an empirical estimate of the cloud base height. The temperature (T_L) pressure (P_L) and height (Z_L) of the LCL is obtained using following equations (Bolton 1980; Stull 1988; Anurose et al., 2016):

$$T_L = \frac{2840}{3.5\ln(T_{30m}) - \ln(Pw_{30m}) - 4.805} + 55 \qquad (1)$$

$$P_L = P_{30m}\left[\frac{T_L}{T_{30m}}\right]^{3.5} \qquad (2)$$

$$Z_L = -H \ln(P_L/P_0) \quad (3)$$

where T_{30m}, P_{30m} and Pw_{30m} are temperature, pressure and water vapor pressure at 30 m height, respectively, P_0 is surface pressure and H is scale height taken as 7.5 km (Wallace and Hobbs 2006).

(~Line 555-575) The LCL generally occurs either below or at the CBL and RL except a few times when it occurs above the CBL and RL (Figs. 11d-e). The cases when the LCL occurs above the CBL or RL, clouds may not be generated by the processes driven by the ABL and can be formed due to large scale-dynamics (Anurose et al., 2016). We observed no relationship between the SBL and LCL (Fig. 11f). For the SBL case, as the vertical motion is inhibited, the relationship between the LCL and SBL is irrelevant (Anurose et al., 2016). Anurose et al., (2016) also studied the relationship between the CBL height and the LCL over the coastal station, Thiruvananthapuram (8.5◦ N, 76.9◦ E), they did not observed any relationship. However, the LCL over Thiruvananthapuram is found to higher than ABL for a majority of the database in contrast to Gadanki.

(~Line 620-629) When the CTH is within ± 0.5 km of the ABL_{CR}, LCL occurs mostly below the ABL, except a few cases when it coincides with either the ABL or CTH (Fig.13a). When the CTH is below 0.5 km of the $ABL_{CR,}$ the LCL again occurs mostly below the ABL but generally coincided with the CTH (Fig.13b). In this case, the LCL sometimes also occurs above the CTH. The clouds occurring below the ABL could be the shallow clouds, in such cases LCL representing the cloud base may occur near to the CTH. However, it is to be noted that the CTH represents the cloud condition for the area averaged over 0.25° latitude X 0.25° longitude regions, whereas the LCL indicates the cloud base exactly over the observation site. Thus, the LCL may not always agree with the CTH when the cloud is not extended over the larger area. For the cases when the clouds occurring above 0.5 km but below 6.0 km of the ABL_{CR}, the LCL mostly occurs either below the ABL or generally coincides with the ABL (Fig 13c).

Comment 3) You can calculate the equivalent potential temperature and saturation equivalent potential temperature from Bolton (1980) and then further calculate the convective available potential energy (CAPE) and Convective Inhibition (CINE). These are very important quantities and will make the article very robust.

Reply 3: Certainly appreciate the helpful suggestion; however, carrying out this is beyond the scope of the present work. We will take up these works in the future as follow-up studies.

Changes in manuscript 3: No changes made in the revised manuscript.

Comment 4) You have reported the Cloud top heights (CTH) from the satellite measured TBB. It will be great if you report the cloud base height and cloud top heights from the radiosondes themselves. The RH measurements will tell you when the sensor is passing through cloud layers. The derived cloud base height then can be added to figure 8 and 10. You can then classify the thermodynamic structure based on cloud thickness rather than cloud top heights.

Reply 4: Following the method of Wang and Rassow (1995), the cloud base height is obtained from the relative humidity (RH) measurement as shown in the Figure below. The time series of the cloud

base height whenever detected using RH in general agree with the cloud top height obtained using TBB data except during deep convection events. However, as the criteria for fixing the cloud base and top heights using the RH data has not been finalized for the tropical clouds occurring over this region, we have preferred satellite derived CTH data in this study. For instance, during December 18-21, 2013, when deep convection occurred, RH has never exceeded 60% and indicates no cloud based on the RH measurement. The detailed study pertaining to the identification of the vertical structure of cloud using RH and its comparison with one identified using satellite brightness temperature data we plan to carry out in the future.

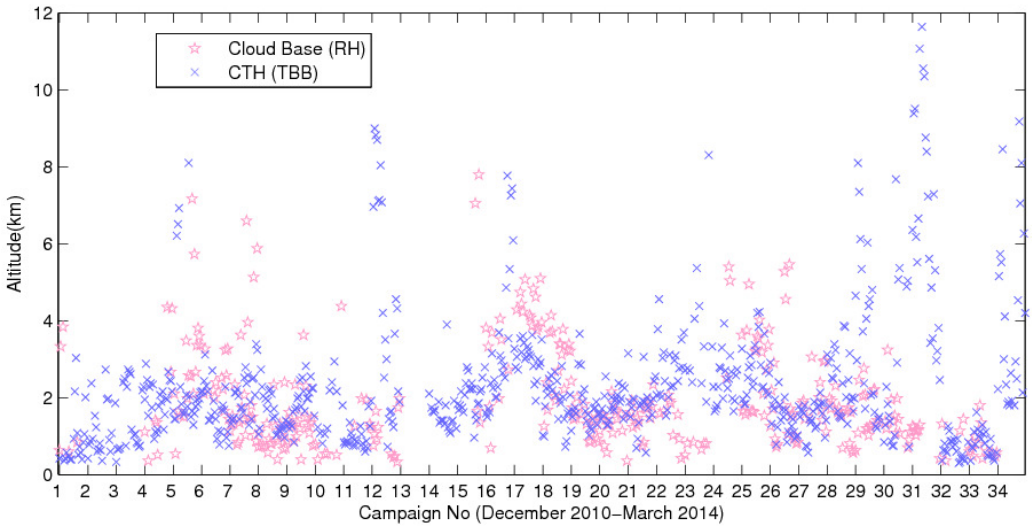

Figure: Time series of the Cloud base height obtained from RH measurement and Cloud top height obtained using satellite measurements.

Wang, J. and Rossow, W.B.: Determination of cloud vertical structure from upper-air observations. Journal of Applied Meteorology, 34(10), pp.2243-2258, 1995.

Changes in manuscript 4:

(~Line 709-711) As suggested by Wang and Rassow (1995), the various cloud layers can be obtained utilizing the RH data (Wang and Rassow, 1995). However, as the criteria for fixing the cloud base and top heights using the RH data has not been finalized for the tropical clouds occurring over this region, we have preferred satellite derived CTH data in this study.

Comment 5) You have made a very good attempt at classifying the BL structure as convective+residual, stable, stable+convective etc. It will be very nice if you can make a cartoon similar to Figure 9.21 of Wallace and Hobbs book with actual values you have for the summer and winter seasons. Thanks.

Reply 5: Thanks for nice suggestion. We have added a cartoon representing the diurnal evolution of the ABL during the summer and winter seasons similar to Wallace and Hobbs (2006).

Wallace J.M., Hobbs, P.V.: Atmospheric science an introductory survey, second edition. International Geophysics series, Acadamic Press 92, 483 pp, 2006.

Changes in manuscript 5:

(~Line 576-592) Figures 12a and 12b show the schematic representation of the diurnal evolution of the mean ABL from 11:00 IST on the first day to 11:00 IST on the second day during the winter and summer monsoon seasons, respectively. The diagram is generated from the seasonal mean ABL height data presented in Figs.10a and 10b. The vertical cross section of the ABL characterizing the seasonal mean CBL, SBL, RL, and entrainment zone (E.Z.), capping inversion and the LCL obtained from the observed data over Gadanki. The schematic diagram represents the typical evolution of the boundary layer, consistent to the diagram presented in the Stull (1988) and Wallace and Hobbs (2006). The CBL during the winter evolves slowly when compared to summer monsoon season in which the ABL growth is rapid. The SBL starts to form well before the sunset during both seasons; however, it remains persistent, even after the sunrise only during the winter season. During the winter, the RL remains almost constant throughout the night. However, during the summer, the RL rapidly decreases as the night passes. The capping inversion during the summer is thicker when compared to the summer monsoon. We have also shown the seasonal mean LCL which occurs within the CBL and RL during both seasons. Note that the transition regions (from the CBL to RL during evening transition and the RL to CBL during morning transition) cannot be accurately represented with available time resolutions. Thus, the part of the CBL after the sunset and the part of the RL after the sunrise may not possess any meaning. This schematic diagram clearly represents the typical (Fig.4), annual mean (Fig.9) and seasonal mean (Fig.10) characteristic of the ABL.

Minor concerns:

1) The shades are not visible in the Table.

Reply 1: Changed to italic font along with shades.

2) Line 15: Please add MSL after lat, lon

Reply2: Added.

3) Line 22: I would say "constant" rather than "steady".

Reply 3: Changed.

4) Line 36: You mean Stull 1988 not 1998.

Reply 4: Corrected.

5) Line 39: You mean to say "convective" and not "convection"

Reply 5: Changed.

6) Line 45-60: what about the role of shear and radiation.

Reply 6: Added to L59 in the revised manuscript.

7) Line 65-70: Might be good to refer to Schmidt and Niyogi.

Reply 7: Cited.

8) Line 74: You mean to say "remote sensing" not "remote sounding".

Reply 8: Corrected.

9) Line 90: "launches" and not "launchings"

Reply 9: Corrected.

10) line92: "has" and not "have"

Reply 10: Corrected.

11) Line 97: Please list the full-form of the acronum CAWSES

Reply 11: Added.

12) Line 165: It might be good to mention that the reported drift is below 4km.

Reply 12: Mentioned.

13) Line 425-426: Please rephrase. "Attains" is misleading.

Reply 13: Changed.

14) Figure 3 legend is incorrect.

Reply14: Corrected.

15) Figure 4: I believe you have listed the lines for sunset and sunrise backwards.

Reply 15: Yes, Corrected.

16)Figure 6a: Why do you have two black bars surrounding the yellow bars.

Reply 16: As black bar is wider than yellow bar, appears as two black bars. Black bar is kept back of yellow bar. As suggested by reviewer# 1, we have modified figure 6a as figure 10 in the revised manuscript.

Diurnal variability of the Atmospheric Boundary Layer height over a tropical station in the Indian Monsoon Region

Sanjay Kumar Mehta[1], Madineni Venkat Ratnam[2], Sukumarapillai V. Sunilkumar[3], Daggumati Narayana Rao[1], and Boddapaty V. Krishna Murthy[1]

[1]SRM Research Institute, SRM University, Kattankulathur-603203, India
[2]National Atmospheric Research Laboratory, Gadanki-517112, India
[3]Space Physics Laboratory (SPL), VSSC, Trivandrum-695022, India

Correspondence to: Sanjay Kumar Mehta (sanjaykumar.r@res.srmuniv.ac.in; ksanjaym@gmail.com)

Abstract. The diurnal variation of atmospheric boundary layer (ABL) height is studied using high resolution radiosonde observations available at every 3-h intervals for 3 days continuously from 34 intensive campaigns conducted during the period December 2010-March 2014 over a tropical station Gadanki (13.5°N, 79.2°E, 375 m), in the Indian monsoon region. The heights of the ABL during the different stages of its diurnal evolution, namely, the convective boundary layer (CBL), the stable boundary layer (SBL), and the residual layer (RL) are obtained to study the diurnal variability. A clear diurnal variation in 9 campaigns is observed while in 7 campaigns the SBL does not form for the entire day and in the remaining 18 campaigns the SBL form intermittently. The SBL forms for 33%-55% of the time during nighttime and 9% and 25% during the evening and morning hours, respectively. The mean SBL height is within 0.3 km above the surface which increases slightly just after midnight (0200 IST) and remains almost constant till morning. The mean CBL height is within 3.0 km above the surface which generally increases from morning to evening. The mean RL height is within 2 km above the surface which generally decreases slowly as the night progresses. The diurnal variation of the ABL height over the Indian region is stronger during the pre-monsoon and weaker during winter season. The CBL is higher during the summer monsoon and lower during the winter season while the RL is higher during the winter season and lower during the summer season. During all seasons, the ABL height peaks during the afternoon (~1400 IST) and remains elevated till evening (~1700 IST). The ABL suddenly collapses at 2000 IST and increases slightly over night. Interestingly, it is found that the low level clouds have an effect on the ABL height variability, but not the deep convective clouds. The lifting condensation level (LCL) is generally found to occur below the ABL for the majority of the database and they are randomly related.

1 Introduction

The atmospheric boundary layer (ABL) is the lowest layer of the troposphere in which the flow field is directly influenced by the interaction of the Earth's surface at a response time scale of about an hour or less (Stull 1988, Garratt, 1994). The importance of the ABL stems from the fact that it is the gateway for the pollutants and anthropogenic emissions, moisture, heat and momentum fluxes to the free atmosphere. Rapid transport in the ABL takes place in order to achieve the radiative balance between the surface and the free atmosphere. The ABL is the largest sink for atmospheric kinetic energy. The ABL height is a key parameters, providing a length

Deleted: i

Deleted: steady

Deleted: D

Deleted: the

Formatted: Font: (Asian) +Body Asian (MS Mincho)

Deleted: A

Deleted: 9

Deleted: earth

Deleted: one

Deleted: of the

Deleted: which

Deleted: es

scale for the vertical extent and concentration of atmospheric pollutants, convective activity, and cloud and fog formation (Deardorff, 1972; Holtslag and Nieuwstadt, 1986; Seibert et al., 2000; Konor et al., 2009). The diurnal variability is a dominant feature of the ABL, which plays an important role in the exchanges of heat, momentum, moisture, and chemical constituents between the surface and free atmosphere.

Depending on the physical process, the diurnal pattern of the ABL is mainly classified into three major layers: the convective boundary layer (CBL), the stable boundary layer (SBL), and the residual layer (RL) (Stull, 1988; Garratt, 1994).The CBL evolves during the daytime just after the sunrise due to convective turbulence (thermals of warmer air) associated with entrainment zone, a stable layer, on its top. Just before the sunset and during night, as the thermals cease to develop, the CBL collapses and the SBL form due to fast cooling of the surface. Even though thermals cease to develop during nighttime the mean state variables remain nearly the same as the former CBL, creating the RL associated with capping inversion layers, a stable layer, on its top. Thus, the RL is disconnected from the ground by underlying SBL having no source of turbulence generation for its maintenance, rather turbulence decays homogeneously in all directions. One aspect of the RL that has been pointed out as being important for the diurnal evolution of the ABL is that it provides the potential for "explosive growth" of the ABL as a CBL forms in the morning and grows into the RL. Generally, the mean ABL height lies between 0.03-3.0 km above the surface (Stull, 1988). However, the CBL can be as high as ~ 5.0 km during a midsummer day in low-latitude deserts and as low as ~0.5 km over the ocean. The SBL height generally is less than 0.5 km above the surface (Garratt, 1992).

As daytime the surface flux (the convectively-induced turbulence) due to solar heating is stronger than night-time surface flux (wind-induced turbulence) due to surface friction causes diurnal variation in the ABL. However, diurnal variability of the ABL is not only determined by the variabilities in the surface fluxes, but also on meteorological conditions such as the presence of the clouds, horizontal advection of air and subsidence from aloft. These forcings considerably affect turbulence development and the growth of the ABL. As, for example, the presence of clouds greatly influences the turbulent structure due to local radiative heating or cooling. The diurnal variation is generally strong, mainly over land in the absence of any upper level cloud and at the time of year when surface temperatures are the highest (Angevine et al., 2001).

The ABL height is often determined from the vertical profiles of temperature, humidity, and wind components obtained from radiosonde measurements (Schmid and Niyogi, 2012). Most of the routine radiosondes only operate twice a day at 0000 and 1200 UTC, which are not suited well to study the diurnal variations of the ABL height. Thus, there have been only a few studies on diurnal variability of the ABL height (Angevine et al., 2001) mainly due to non-availability of the required measurements with adequate time resolution. High resolution radiosondes launched at sufficiently close time intervals (less than 1-h) can provide direct information on diurnal variability of ABL height. Liu and Liang (2010) studied the climatology of the ABL height diurnal cycle, using fine-resolution soundings launched at intervals ranging from 1-12 hours collected in 14 major field campaigns around the world. They found a strong diurnal cycle, both over land and oceans, whereas the cycle is weak over ice. Seidel et al., (2010) using routine radiosondes over the globe found significant differences in day and night ABL heights. In an another study, Seidel et al., (2012) reported the seasonal pattern in the diurnal cycle of the ABL using 3 hourly ERA-Interim data and 6 hourly climate models outputs over the continental United States and Europe. There are several case studies focusing on the diurnal structure of the boundary layer and the mechanism responsible for its formation over different regions of the globe. Brill and Albrecht, (1982)

Deleted: on

Deleted: forms

Deleted:

Deleted:

Formatted: Font: Not Italic

Deleted: m

Deleted: D

Formatted: Don't adjust right indent when grid is defined, Don't adjust space between Latin and Asian text, Don't adjust space between Asian text and numbers

Formatted: Font color: Text 1

Deleted: campaign

presented the diurnal variation of the cloud fraction and trade-wind inversion base height using the data collected from various ships and aircraft. May et al., (2012) have studied the diurnal variation of convection, cloud, radiation, and boundary layer structure in the coastal monsoon environment (Darwin, Australia). Santanello et al., (2007) has studied the feedback of soil moisture dryness on the development of the convective boundary layer over the southern Atmospheric Research Measurement Program–Great Plains Cloud and Radiation Testbed (ARM-CART) sites. During a clear sky day Hashiguchi et al., (1995a) observed boundary layer radar echo indicating the ABL height. Hashiguchi et al., (1995b) further observed that the boundary layer radar detects diurnal variation of the ABL both at the equatorial and midlatitude regions. During the summer over a midlatitude glacier, the diurnal and vertical and horizontal structures of the boundary layer were found to be dominated by persistent glacier winds forced by gravity (Van den Broeke, 1997).

Recently, various remote sensing systems such as lidar (Tucker et al., 2009), sodar (Shravan Kumar and Anandan, 2009), wind profiler (Kumar and Jain, 2006; Bianco et al., 2011), Radio Acoustic Sounding System (RASS) (Clifford et al., 1994; Chandrasekhar Sarma et al., 2008), ceilometer (van der Kamp and McKendry, 2010) have been developed for continuous direct measurements or estimates to study the diurnal variation of the ABL height (Seibert et al., 2000). Sodar can generally provide the SBL height but not always the CBL height due to inadequate height coverage. The lidars make use of aerosol extinction profiles and can provide information on diurnal variability of the ABL height. Using network of wind profilers located in California's Central Valley, Bianco et al. (2011) studied the diurnal evolution of the CBL which attains maximum height 3-4 h before the sunset. A few studies on the different ABL regimes (CBL and SBL) and their evening transition have been carried out using various remote sensing instruments located at Gadanki (Kumar and Jain, 2006; Basha and Ratnam, 2009; Kumar et al., 2012; Sandeep et al., 2015).These studies show that the mean CBL height is within 3.5 km and the mean SBL height lies below 0.6 km above the surface and their transition from the CBL to the SBL occurs about one and half hour before the sunset. However, the complete diurnal variation of the ABL height has not been reported either using single instrument or a combination of two or more in the above mentioned studies.

Over Gadanki (13.45°N, 79.2°E), a tropical location in the Indian monsoon region high resolution GPS radiosonde launches were carried out in 3-h intervals for three consecutive days in each month during the period December 2010- March 2014. Making use of this dataset, first time complete diurnal variability of the ABL height and their classification into different ABL regimes such as the CBL, SBL and RL during different seasons and effect of the cloud in its diurnal structure has been studied and the results are presented in this paper. Section 2 describes the data and methodology, results are presented in section 3, and in section 4 discussion and concluding remarks are presented.

2 Data and Method of analysis

2.1 GPS Radiosonde data

As part of Tropical Tropopause Dynamics (TTD) experiment under Climate and Weather of Sun-Earth System-India (CAWSES-India) program, intensive campaigns of high resolution GPS radiosonde were conducted to study the diurnal variability of the ABL over a tropical station, Gadanki, located at 375 m above mean sea level. The radiosondes were launched at 3-h intervals for 3 consecutive days in each month from December 2010 to

Deleted: ¶
Deleted: sounding
Deleted:
Deleted: ing
Deleted: a
Deleted: the
Deleted: s
Deleted: of
Deleted: (of the ABL)
Deleted: have
Deleted: continuously

March 2014, except during March 2011, December 2012, January-February 2013 and April 2013. Each campaign started at 1100 IST (=UTC+0530) on day one and ended at 0800 IST on the day four. Table 1 shows the dates of radiosonde launchings. Most of the observations are conducted during non-rainy days except two during 01:00 IST-02:00 IST on 18 August 2011 and 14:00 IST-20:00 IST on 21 August 2012, with total rainfall about 47 mm and 46 mm, respectively. In total 764 profiles of temperature, pressure, relative humidity and horizontal wind are obtained from the 34 campaigns. These data are collected using 'Meisei RD-06G' radiosonde observations sampled at 10 m (sampled at 2 Sec intervals) under the TTD campaigns (Ratnam et al., 2014). The observed data set is gridded uniformly to 30 m altitude resolution interval so as to remove any outliers arising from random motions or very high frequency fluctuations but the same time to retain the ABL signature. Note that gridding these data to coarser resolution (e.g. 100 m) smooths out the ABL detection, especially the SBL, which lies generally below 0.5 km above ground level. Quality checks are then applied to remove any further outliers arising due to various reasons to ensure high quality in the data (Mehta et al., 2011).

Deleted: at

Formatted: Font: (Asian) +Body Asian (MS Mincho), (Asian) Japanese

2.2 Infrared Brightness Temperature (TBB) data

In order to understand the role of clouds especially low-level clouds occurring around the ABL cloud top temperature (CTH) is estimated using Infrared Brightness Temperature (TBB) obtained from the Climate Prediction Centre, NOAA which available at a time resolution of one hour and at a spatial resolution of 0.03^{o} X 0.03^{o}. This is globally-merged, full-resolution (~4 km) IR data formed from the ~11 micron IR channels aboard the GMS-5, GOES-8, Goes-10, Meteosat-7 and Meteosat-5 geostationary satellites. The data have been corrected for zenith angle dependence to reduce discontinuities between adjacent geostationary satellites. For this study, we averaged the TBB data into 0.25^{o} latitude X 0.25^{o} longitude around Gadanki and collected for every three hours during each campaign. The cloud top height is obtained as altitude corresponding to averaged TBB from radiosonde temperature profiles.

Deleted:

Deleted: is used to infer the cloud top height (CTH)

2.3 Method of analysis

Altitude profiles of temperature variables and moisture variables obtained from radiosonde observations are used to estimate the ABL height based on different methods. Seven different methods, two using the temperature profile, three using the moisture profile and two a combination of temperature and moisture are adopted to estimate the ABL height in each sounding. The temperature variables are dry air temperature (T), potential temperature (θ) and moisture variables are relative humidity (RH), specific humidity (q) water vapor pressure (P_w). A combination of both temperature and moisture variables are virtual potential temperature (θ_v) and radio refractivity (N). The ABL height is generally identified as the location of (1) the maximum vertical gradient of one of the variables: T, θ, and θ_v or (2) the minimum vertical gradient one of the variables: RH, q, P_w , and N (Sokolovskiy et al., 2006; Basha and Ratnam, 2009; Seidel et al., 2010; Chan and Wood, 2013) below 3.5 km above the surface. We limited the altitude region to 3.5 km, following Chan and Wood (2013) who used GPS radio occultation refractivity data to study the seasonal cycle of the ABL over the globe. The upper limit 3.5 km is selected in order to avoid the midlevel inversions, if any. When more than one peak in the gradient occurs below 3.5 km, the lowest peak having a value greater than 80% of the main peak is considered as the ABL top. As suggested by Ao et al. (2012), the gradient based ABL definitions are most meaningful when they are large in magnitude relative to the average gradient. They defined the "sharpness parameter" as

$X'_S = |-X'_{min\ or\ max}/X'_{RMS}|$ where X is moisture or temperature variables and X'_{RMS} is the root-mean square (RMS) value of X' over the altitude range 0-3.5 km. If $X'_S \geq 1.25$ it is considered that ABL is well defined. In the case of SBL the gradient at the top of the residual layer is much stronger than that of the gradient at the SBL. The SBL is generally identified using surface based inversion methods (Seidel et al., 2010). At the SBL, where temperature increases sharply, the temperature gradient shows a maximum value immediately just above the surface, but not at the actual level where the temperature reverses from the positive to negative gradient. In the present study, the SBL is identified as the level of maximum temperature below 0.9km. The upper limit for the SBL height identification is based on Kumar et al. (2012), who observed the maximum wind speed (sporadic region) deep enough up to~0.9 km. The method to obtain the RL is similar to that of the CBL.

Following the above criteria, we have obtained the CBL, SBL and RL heights during each campaign listed in Table 1. Out of 764 profiles, 17 profiles are rejected due to bad data quality. In the night time two types of profiles are observed; one in which the SBL is present and other in which the SBL is not present. The profiles for which the SBL is defined, are further subdivided into two cases; i) with the RL not defined and ii) the RL defined. As the observations are at 3-h intervals, actual changes happening during the morning transition (MT) and evening transitions (ET) during the course of diurnal cycle might not have been captured. Sandeep et al. (2015) have made a comprehensive study on the transitory nature of the ABL during ET over Gadanki. They found that the transition follows a top-to-bottom evolution. Note that the mean sunrise time is about 0545 IST (0630 IST) while sunset time is about 1830 IST (1745 IST) during the summer (winter) over Gadanki.

The lifting condensation level (LCL) is defined as the height at which an unsaturated air parcel becomes saturated (RH >100%) when it is cooled by dry adiabatic lifting (Wallace and Hobbs, 2006). It provides an empirical estimate of the cloud base height. The temperature (T_L) pressure (P_L) and height (Z_L) of the LCL is obtained using following equations (Bolton 1980; Stull 1988; Anurose et al., 2016):

$$T_L = \frac{2840}{3.5\ln(T_{30m}) - \ln(Pw_{30m}) - 4.805} + 55 \quad (1)$$

$$P_L = P_{30m}\left[\frac{T_L}{T_{30m}}\right]^{3.5} \quad (2)$$

$$Z_L = -H\ln(P_L/P_0) \quad (3)$$

where T_{30m}, P_{30m} and Pw_{30m} are temperature, pressure and water vapor pressure at 30 m height, respectively, P_0 is surface pressure and H is scale height taken as 7.5 km (Wallace and Hobbs 2006).

3 Results

3.1 Topography, balloon trajectory and mean wind pattern over Gadanki

Figure 1a shows the seasonal mean trajectories of balloon below 4 km and locations of balloons at 4 km during different seasons launched over Gadanki for the period December 2010-March 2014. Gadanki is surrounded by hills of maximum height of 500-600 m above the mean sea level. Towards west of the Gadanki is the chain of the Nallamala hills with height about 800-1000 m and east side of it is flanked by Bay of Bengal. Note that Gadanki is a far inland station (~120 km away from the Bay of Bengal coast) and hence does not have any local effect due to the sea. The balloon generally has drifted about 0.1° and 0.2° in latitude and longitude, respectively below 4 km. It can be seen that balloon ascends almost vertically and has drifted towards the southwest

Formatted: Indent: First line: 0 cm
Formatted: Font: Times New Roman
Deleted:

direction during the winter season (DJF; December- January-February) while during summer monsoon season (JJA; June-July-August) they are drifted mostly towards southeast direction. During pre-monsoon (MAM; March-April-May) balloon ascends almost vertically up to 1 km and drifts southward above up to4 km. In the post-monsoon months (SON; September-October-November) it ascends almost vertically up to 2-3 km and change direction towards southeast.

Figures 1b-c show the seasonal mean zonal (U) and meridional (V) winds, respectively, obtained using averaging horizontal wind data observed during the period December 2010- March 2014. Within the ABL, it can be seen that the zonal winds are mostly easterly during the winter and pre-monsoon while westerly during the summer monsoon and post monsoon and the meridional winds remain southerly throughout the year. During the summer monsoon season, low level westerly jet (LLJ) core of 10 m/s at 1 km is clearly evident.

3.2 Identification of the ABL (CBL and SBL) from temperature and moisture profiles

Figure 2 shows the typical profiles of the temperature variables T, θ, θ_v and the moisture variables RH, q, P_w and N observed at 1100 IST on 8 February 2011 to identify the CBL. Note that these profiles are observed in clear sky conditions (TBB ~295 K). It can be seen that the CBL is capped by the inversion layer of thickness 0.150 km where a sharp increase in temperature and a sharp decrease in the moisture variables occur. The base of the entrainment zone is at 0.69 km above the ground level, which is defined as the top of the CBL. Within the CBL, θ, θ_v, and q and P_w are almost constant with altitude signifying that the air is mixed or having a tendency towards vertical mixing due to the action of the turbulence, a characteristic of the 'mixing layer' (Seibert et al., 2000). Above the CBL and within the entrainment zone T, θ and θ_v increase sharply by about 1.5 K, 3.0 K and 2.0 K, respectively, and moisture variables (RH, q, P_w and N) decrease sharply by about 6 times. At the top of the entrainment zone, θ_v coincides with θ as water vapor concentration becomes very small. These sharp changes at the CBL top are easily captured by the gradient of the temperature and moisture variables as shown in Figs. 2b and 2d, respectively. Both the maximum gradient of the temperature variables and the minimum gradient of the moisture variables identify the CBL height quite well.

Deleted: convective

As mentioned earlier, after sunset (in the nighttime) the identification of the SBL is not as easy as the identification of the CBL, mainly because of the absence or delay in the formation of the surface inversion due to weak surface cooling. Therefore, whenever the SBL is not present the ABL is represented as the RL. Typical examples of identification of the SBL are shown in Figs. 3a-3l for three different types of nighttime temperature (T, θ and θ_v) and moisture (RH, q,P_w and N) profiles and their corresponding gradient profiles indicating the presence of the SBL but not the RL, both the SBL and the RL, not the SBL but the RL, respectively. The temperature and moisture profiles and their corresponding gradient profiles observed at 0200 IST on February 9, 2011 show the evolution of the SBL only but not the RL (Figs. 3a-3d). The gradients of temperature profiles and moisture profiles shown in Fig. 3b and Fig. 3d are offset by scale 10. These profiles are observed during fair weather conditions (TBB ~ 295 K). The top of the SBL identified based on the surface based the inversion (SBI) in the T is indicated as a horizontal dashed line in Fig 3a. The SBL is identified at 0.39 km above the ground level. Within the SBL both θ and θ_v increase steeply. The temperature gradient profiles show a maximum gradient at the surface which steeply decreases within the SBL (Fig 3b). The moisture profiles (Fig. 3c) also show a steep decrease within the SBL. However, their gradients (Fig. 3d) show a negative peak at 0.18 km observed at a lower height when compared to top of the SBL. The negative gradient peaks in the moisture

variables are denoted as open circles. These sharp changes in the moisture variables in the SBL are indicative of inversion forming adjacent to the surface similar to the formation of entrainment zone aloft in the development of the CBL. Thus, one can also identify the height of the SBL based on moisture gradient peaks (especially when temperature observation is not available) near the surface when the RL is absent. However, it becomes difficult when the gradient aloft is strong as will be seen in the later examples.

A similar feature can be noticed in the case of the SBL forming beneath the RL as identified using temperature and moisture variables, shown in Figs. 3e-3h observed at 0200 IST on December 19, 2013. These profiles are observed under deep convective case with the TBB value about 262.3 K and corresponding CTH is 6.67 km. In this case, the SBL based on the SBI is identified at 0.21 km above the ground level (Fig. 3e). The temperature variables increase and moisture variables decrease in the SBL (Figs 3e and 3g), but not as steep as previous profiles shown in Figs. 3a and 3c, respectively. The gradient method identifies the RL top at 1.35 km denoted by open circles as shown in Figs. 3f and 3h. The RL has similar features as the CBL mentioned in Fig 2. One can observe a weak gradient in the moisture variables (Fig. 3h) at 0.30 km. It can be assigned as the top of the SBL defined using the gradient method in the moisture, which is slightly higher than the SBL defined using surface based inversion. However, identification of the negative gradient peak in the moisture profiles becomes difficult when strong RL is present as can be noticed from the next example.

Unlike the above mentioned cases, an example indicating no SBL formation beneath the RL in both temperature and moisture profiles observed at 0200 IST on February 26, 2014 is shown Figs. 3i-3l. In this case, the feature of the RL is similar to that shown in Fig. 2 for the CBL and that shown in Figs. 3e-3h for the RL. Like CBL, it also starts from the surface. By definition the RL is the layer observed above the SBL and hence not considered as the ABL. However, if the SBL is absent as in this case, the RL will be above the surface and it is nothing but nighttime ABL. In a study more similar in concept to ours, Liu and Liang (2010) pointed that such cases are generally identified with near-neutral conditions in the surface layer which they assigned as the neutral RL (NRL) that starts from the ground surface. However, in our study, we refer to it as the RL. Using gradient method, the top of the RL is identified at 1.47 km from the temperature variables and at 1.14 km from the moisture variables. The moisture profiles and its corresponding gradients are disturbed for about 1.0 km above the RL. Unlike the previous examples, the moisture profiles in this case do not sharply decrease. The TBB at 0200 IST on February 26, 2014 is 289.4 K and corresponding CTH of 0.81 km, indicating the presence of the low level fair weather clouds. The RL height difference observed using temperature and moisture variables is difficult to explain, but seems related to the effect of the cloud. The surface moisture is very small and the LCL observed at about 0.6 km indicates that a shallow layer cloud of thickness about 0.2 km decoupled from the surface (Garratt, 1992). The absence of the SBL indicates lack of sufficient surface cooling which could be due to presence of cloud above radiatively warming the surface. It is to be noted that there is a weak gradient present in both temperature and moisture variables at 0.51 km which is very small when compared to the gradient at the RL. Comparing the moisture gradients below the RL top shown in Fig. 3l with that presented in Fig. 3h, it is inferred that the gradient below the RL may not always be due to surface cooling. Hence, identifying the SBL using moisture variables based gradient method needs caution. Thus, in the present study, we preferred the identification of the SBL based on the SBI only.

Deleted: is

3.3 Typical diurnal variation of the ABL

From the previous typical examples presented for particular times, it is observed that the ABL identified using temperature and moisture variables independently agree fairly well. Thus, any one temperature variable and any one moisture variable are sufficient to document the ABL variation. It is also observed that the ABL heights are well identified during different cloudy conditions. Thus, hereafter we only examine T, θ_v, q and N for the analysis. θ and RH and P_w are dropped from further analysis as they are related to θ_v and q, respectively. The typical examples of the three hourly variations of the CBL, SBL, RL, CTH and the LCL observed over three days are shown in Figs. 4a-4d for four different types of diurnal variation indicating formations of well-defined SBL, delayed SBL, no SBL, and intermittent SBL, respectively. Figs. 4a-4d also show four different cloudy conditions occurring around the ABL, far above (deep convection) the ABL, below the ABL and just above the ABL, respectively. First three (Figs. 4a-4c) panels show the complete 3 days observations for which the typical examples of the particular times have been described earlier in Fig 2 and Fig 3. Note that the diurnal variability of the CBL and RL is identified based on T, θ_v, q and N variables, while the SBL is identified using T only.

Figure 4a shows the perfect diurnal evolution of the ABL for all the 3 days observed during February 8-11, 2012 (see supplementary Fig. S1, which depicts the corresponding vertical profiles T, q and N along with TBB and CTH). The CBL height just before noon (1100 IST) is at height 0.69 km on the first day, which further grows to height 1.2 km during afternoon (1400 IST) owing to the maximum surface heating and remains at the same height till evening (1700 IST) just before the sunset (1816 IST). During this time ET takes place and development of the SBL started at height 0.48 km at 2000 IST, which descends slowly during its nighttime evolution to the height 0.15 km at 0800 IST on the second day. Due to development of convective turbulence after the sunrise (0639 IST), the SBL is in the stage of the disappearance after 0800 IST, probably indicating the activity of MT. During the second and third days, the evolutionary feature of CBL and SBL are similar to that on the first day; however, they show large day to day variability. The CBL was not identified either by using moisture or by temperature variables at 1100 IST on second day (Fig. S1). Either clear sky conditions or the CTH below the CBL is observed during the first and third days (TBB ~ 295 K). During the second day, TBB reduced by about 10 K indicating presence of low level clouds with CTH at 2.5 km. The diurnal variation of the ABL shows the CBL at the same height using all the variables on the first day, but they differ on the second and third days. The CBL height from the minimum gradients of q and N are exactly same, indicating the dominance of the moisture part in the N when compared to T. Similarly, both T and θ_v identify same heights of the CBL and RL indicating dominance of temperature in θ_v when compared to moisture. The RL is not observed on the first night; it appears on the second and third nights, which generally decreases in the course of the night.

A similar example of typical 3 days diurnal variation of the ABL identified using T, θ_v, q and N profiles in which the SBL formation delay observed during December 18-21, 2013 is shown Fig. 4b (see corresponding vertical profiles in Fig. S2). This case is observed during deep convection events. In this case, the CBL height just before noon is at 1.59 km and remains at about the same height till evening. After the sunset, the CBL does not collapse until midnight and the SBL has not formed, indicating delay in ET process. Thus, the ABL heights observed at 2000 IST and 2300 IST are the RL top heights. The SBL appears at height 0.18 km after midnight (0200 IST) and remains at about the same height till morning (0800 IST) on the second day. On the second day, the CBL reappears again at 1.35 km before noon, which became maximum (1.83 km) afternoon and steadily decreases to 1.53 km at 2000 IST. The ET process again delayed and the SBL did not form until just before the

Deleted: and

Deleted: It is observed that t

Deleted:

midnight on the second day. On the third day, the CBL varies in similar fashion as on the second day but this time the ET process was not delayed and the SBL formed on 2000 IST. On the third night the SBL was detected at a height about 0.45 km. Note that both the temperature and moisture profiles show wave like feature during 2000 IST-0800 IST on third night could be either due to strong horizontal advection or due to gravity wave propagation (Fig S2) which will be examined in a separate study. The RL during all three days remain about the same height in contrast to previous example where it decreases as the night progresses.

The TBB lies between the range 285 K to 218 K corresponding to the CTH about 2.46 km to 11.6 km, respectively. By the first day (December 18, 2013) to the evening of the third day (December 20, 2013), deep convection prevails with the CTH above 6 km except a few occasions when it lowers down to about 3.0-4.0 km. From midnight of the third day CTH observed below 3.0 km, during which T, q and N were observed disturbed (Fig S2). The delay in the ET processes seems related to warming caused by cloudy skies, which might have resulted in a delay of the surface cooling during the early part of night of first and second day. However, it must be noted that presence of the clouds could be one possible reason as there as occasions when the SBL forms even in the presence of the clouds. Hence, the delay in the ET process cannot be entirely explained by the longwave effect. It can be seen that, during the deep convection case, the ABL identified using different moisture and temperature variables is the same.

Another typical 3 days variation of the ABL, where the SBL is not formed throughout the observation period and when the cloud lying below the ABL as shown in Fig 4c is observed during February 24-27, 2014 (See Fig S3 for vertical profiles). Thus, during nighttime only the RL is defined which is above the surface and considered as nighttime ABL. None of the temperature profiles show the evolution of the SBI (Fig S3). The ABL is at about 2.0 km (1100-1700 IST) which descends down to height 1.14 km (2000 IST) and to 0.66 km (2300 IST) following ET before midnight on the first day. The CTH indicates the presence of low level cloud at about 1.0-1.5 km since the evening of the first day to early morning of the second day. During these cloudy days, the ABL heights (~1.5 – 2.5 km) are higher than when compared to the ABL height (0.6-1.5 km) determined during clear sky days. An example of the typical 3 days variation of the ABL, where SBL is defined intermittently and when cloud lying above the ABL is shown in Fig 4d observed during May 29-June 01, 2012 (See Fig. S4 for vertical profiles). By intermittent is meant the SBL defined for a few times and not the whole night. In this case, the TBB lies between the range 290 K to 276 K corresponding to the CTH about 1.96 km to 3.60 km, respectively. The CTH is always above the ABL. On the first day, the SBL does not form and the ABL is almost at about the same height till the evening of the second day. On second and third nights the SBL formed for sometimes. In all the above cases, the SBL either has decreased after midnight or remained constant. These two types of the SBL are somewhat equivalent in types reported by Kumar et al., (2012). During clear-sky conditions, the constant and decreasing SBL height after midnight are generally accompanied by steady and unsteady winds (Kumar et al., 2012).

The typical diurnal variation of the LCL for the four different cases of the clouds is shown in Figures 4a-d. In general, it is observed that the LCL forms below the ABL (CBL+RL) except a few cases. During February, 8-11, 2011, the LCL occurs just above the CBL (Fig. 4a) but below the RL. During the second day when the CTH occur at 2.4 km, the LCL also forms near to it. However, the LCL also is higher than the CBL on the first day and the third day, when the CTH is very low. It indicates that the LCL and CTH are not always related. In the case when deep convention is observed during December, 18-21, 2013, the LCL shows nice diurnal cycle as the

Deleted: does

Deleted: ,

Deleted: till

Deleted: 0

ABL (CBL+SBL) (Fig. 4b). During February 24-27, 2014, the case when the CTH is occurring below the ABL, the LCL also occurs below the ABL and at or around the CTH (Fig. 4c). During May 29-June 01, 2012, when the CTH is well above the ABL, the LCL remains almost constant and varies in a similar way as the CBL and RL (Fig. 4d). From these typical cases, it appears that the ABL and the LCL are sometimes closely related and sometimes randomly, a detail comparison of the LCL with different ABL regimes is presented in the later section.

Deleted: ¶

3.4 Correlation analysis

The typical examples of the SBL, CBL and RL identification shown in previous section reveal that the different methods agree well except in a few cases. In order to see the overall correlation of the CBL and RL heights detected from T, θ_v, q and N, a statistical comparison between them has been made as shown in Fig. 5. The total number of observations available during daytime (0800 IST -1700 IST)) is 379. Out of them, the CBL is defined in 360 profiles (see Table 1), in 18 profiles the CBL is not defined and one profile is rejected due to bad data quality. The total number of observations available during nighttime (2000 IST-0500 IST) is 385. Out of them, the RL is defined in 320 profiles as listed in Table 1, in 49 profiles the RL is not defined and 16 profiles are rejected due to bad data quality during the quality check process. Figs. 5a-5d show the scatter plots of the CBL heights obtained using four different methods.

The correlation between the CBL heights obtained from T and θ_v (r = 0.97) (Fig. 5a) and q and N (r = 0.99) (Fig. 5d) are found to be excellent, which have a standard deviation (SD) of0.16 km and 0.10 km, respectively, suggesting that it can be determined using either of the methods. However, the correlation between the CBL heights obtained from θ_v and q (r = 0.79) (Fig. 5b) and T and N (r = 0.78) (Fig. 5c) though agreeing well, have a large SD of about 0.39 km and 0.38 km, respectively. Several times, the CBL height determined from temperature variables is higher than that one obtained from the moisture variables. There could be various reasons for this disparity, however, whenever the temperature and moisture gradients are sharper or having significant gradients (Basha and Ratnam, 2009), both methods define unique height, but differences occur when they are not so sharp. Seidel et al., (2010) observed no correlation between the ABL heights obtained using T (elevated inversion) and the rest of the methods (θ_v, q, N). Surprisingly, they observed good correlation between θ and moisture variables (q, RH, N), but no correlation with T. In fact, θ mostly depends upon the T variation, so one would expect a good correlation between them as observed in our case.

Figures 5e-5h show the scatter plots of the RL heights obtained using four different methods. Similar to the CBL heights, the RL heights also show excellent correlation between T and θ_v (r = 0.94) (Fig. 5e) and q and N (r = 0.96) (Fig. 5h) with SD about 0.24 km and 0.17 km, respectively. The correlation between RL heights obtained from θ_v and q (r = 0.86) (Fig. 5f) and T and N (r = 0.88) (Fig. 5g) with SD about 0.32 km and 0.27 km, respectively, are comparatively better than the CBL heights. However, unlike the CBL heights, the RL heights estimated using different methods scatter uniformly about the linear fit, indicating that sometimes the RL heights obtained using temperature variables are higher than that of moisture variables and vice- versa. As we have observed excellent correlation between different methods, hereafter rest of the results will be presented using T variable only, because both the SBL and CBL can be easily estimated using this variable.

3.5 Statistics of the SBL, CBL, and RL heights

Before proceeding to the diurnal variation of the ABL, we first document the occurrence statistics of the SBL, CBL and RL and the general nature of their diurnal cycle as shown in Fig. 6. The occurrence of the SBL, CBL and RL and the occurrences of the SBL during different seasons are shown in Fig. 6a and 6b, respectively. SBL forms mainly during nighttime, except a few times during the early evening (1700 IST) and the late morning (0800 IST). The SBL occurrence dominates at nighttime (2300-0500 IST) with occurrence about 50%. At 2000 IST, occurrence of the SBL is only 33%, indicating that delay in surface cooling for about 17% of the times. Over Gadanki, the occurrence of the SBL is less than the occurrence over land in the midlatitude (North America and European regions)(Liu and Liang, 2010). The SBL appeared at 0800 IST for about 25% of the time indicating the dominance of the surface cooling even after (generally 2 hours after) the sunrise. As surface cooling starts well before (generally 2 hours before) the sunset, sometimes (about 9%) SBL also forms at 1700 IST. In general, the SBL occurs more frequently during the winter when compared to the summer monsoon season. Liu and Liang (2010) also observed occurrences of the SBL a few times during midday. However, we have not observed such occurrence over Gadanki. It is interesting to note that SBL at 0800 IST mostly formed during the winter months. During winter, when sunrise is at ~ 0630 IST surface cooling may remain strong till 0800 IST on some days leading to the formation of the SBL. Whereas during the summer monsoon season with sunrise at about 0545 IST, surface cooling may not last till 0800 IST leading to very few occurrences of the SBL at 0800 IST. The CBL and RL occurrences dominate and are evenly distributed at 3-h intervals during daytime (0800-1700 IST) and nighttime (2000-0500 IST), respectively. In contrast to Liu and Liang, (2010), we observed the uniform occurrence of the CBL at 3-h intervals during daytime.

Figure 6c-6e shows the mean height of the SBL, CBL and RL along with their respective standard deviations between 1100 IST -0800 IST. The mean SBL height varies between 0.16 ± 0.07 km at 2000 IST to 0.29± 0.21 km at 2000 IST. The overall mean SBL is below0.3 km above the surface consistent with the literature (Stull, 1998). After the sunrise, the CBL starts to form which lies between 1.4 ± 0.62 km at 0800 IST to ~ 2.0±0.5 km at 1400 to 1700 IST (Fig. 6b). Overall the mean CBL height is well below the 3.0 km above the surface consistent with the literature (Stull, 1988; Garratt, 1994). The daytime CBL remains prevalent as part of the RL during nighttime, which slightly falls to 1.8±0.67 km at 2000 IST and becomes minimum 1.6±0.55 km at 0200 IST (Fig. 6c).

We examine the probability distributions in order to find out the most probable height at which the SBL, CBL and RL occur in winter, summer monsoon seasons and in the whole year as shown in Fig. 7. Figs. 7a-7c show the SBL height distribution which has a clear peak at 0.15 km in the annual as well as during the winter and summer are lower than the mean SBL height. Both maximum distributions and mean indicates that the SBL heights are within the 0.30 km as consistent with the literature except a few times when SBL forms above it. The mean SBL height shows clear seasonal variation with lower height during the summer than the winter season. Figs. 7d-7f show the CBL height, which has clear peaks at about 2.0 km in the annual and winter season closely coinciding with the mean CBL. During the summer season, the CBL height distribution shows a broad peak between 0.8 km and 2.4 km, and the mean CBL height is slightly higher than that during the winter season. A clear seasonal variation is also observed in the mean CBL height. It also indicates that CBL heights are highly variable during summer monsoon season when compared to winter season. The RL height distribution is similar to the CBL height distribution in the annual and winter peaking at a lower height ~ 1.8 km (Figs. 7g-7h).

During the summer monsoon season, the RL height distribution shows a peak at 0.8 km in contrast to the CBL distribution. Liu and Liang (2010) also observed similar distributions as reported in this study.

We also obtained the distribution of the SBL, CBL and RL for the annual, winter and summer monsoon in terms of the boxplot as shown in the Figs. 8a-c, respectively. The median values the SBL during the annual, winter and summer remain same (Fig. 8a). There are a few outliers whose values are greater than 3 times of the corresponding interquartile ranges (IQR) for the annual and two different seasons. The SBL mostly lies below 0.65 km during the winter and 0.4 km during summer monsoon. The SBL is more variable during the winter than summer monsoon. As mentioned earlier, the CBL is higher and more variable during the summer monsoon than winter (Fig. 8b). Similarly, the RL is also more variable during the summer monsoon than winter (Fig. 8c). In contrast to the CBL, RL is lower during the summer monsoon when compared to winter.

3.6 Diurnal and Seasonal Variation of the ABL height

We have two combinations of the ABL variability; one is the CBL and the SBL denoted as the ABL_{CS} and another is the CBL and the RL denoted as the ABL_{CR}. The diurnal variation of the ABL_{CS} height, ABL_{CR} height, the surface temperature and the LCL height are shown in Fig. 9. The surface temperature is taken from the automatic weather station (AWS) observations over Gadanki. The diurnal variation of the ABL comprises of the CBL observed between 0800 IST and 1700 IST, the SBL at 1700 IST and 0800 IST and the RL observed between 2000 IST and 0500 IST. As mentioned earlier, the mean CBL varies between ~0.5 km and 3.0 km and the mean SBL varies between ~ 0.09 km and 0.6 km. The mean diurnal variation of the CBL and the SBL (ABL_{CS} hereafter) shows that the CBL evolved slowly with time attains maximum height at 1400 IST and either remains constant or decrease slowly till 1700 IST and then collapse to the SBL. The mean variation of the SBL over time is very small. It can be seen that the ET is more abrupt at 1700 IST than the morning rise at 0800 IST consistent to earlier studies (e.g. Liu and Liang, 2010).

The variation of the CBL and RL (ABL_{CR} hereafter) over three days for all the campaigns is shown in Fig. 9b. Note that the CBL variation at 1700 and 0800 IST presented in Fig. 9a is relatively lower because former also includes the SBL observations; especially during 1700 IST and 0800 IST (see Fig 6). It is interesting to note that the RL falls to lower height most of the night and thus, the ABL_{CR} shows a diurnal pattern with maximum height during 1700 IST and minimum during early morning 0800 IST. The observed maximum height of the CBL at 1700 IST is found to be consistent with the general circulation model output (Medeiros et al., 2005). The RL height varies from~0.5 km to ~3.0 km. The RL is present throughout the night during most of the day, which is sustained by the presence of the relatively warm air trapped between two stable layers, RL at the top and recently developed SBL due to surface cooling at the bottom. The trapped warm air slowly becomes cooler due to exchange of heat to the adjoining free atmosphere and gradually intensifying SBL results in the descent of the RL during the course of the night, allowing the turbulence to decrease homogeneously in all directions.

The diurnal variation of the ABL_{CR} shows somewhat similar pattern as the surface temperature (Fig. 9c) and the LCL (Fig. 9d). Both surface temperature and LCL become maximum at 1400 IST and minimum at 0200 IST. The diurnal pattern of the LCL height is similar to the pattern of the surface temperature. The mean LCL height is lower than the CBL and RL height. The higher the surface temperature higher is the LCL and vice versa.

Deleted: observed

Deleted: ¶

Deleted: and

Deleted: 8

Deleted: 8b

Deleted: 8a

Deleted: D

Deleted: a

Deleted: The

Deleted: attains

Deleted: a

Deleted: a

Figure 10 shows the diurnal variation of the ABL height (obtained using *T* variable) and surface temperature during different seasons. We have considered those cases which show the diurnal pattern of the ABL i.e. the formation of the CBL during daytime and SBL during nighttime as well as all those cases whenever SBL forms intermittently (excluding RL). As mentioned earlier, note that the occurrence frequency of the SBL just after the sunset is less than that of later periods at night. It means that the SBL has not formed always immediately after the sunset. Several times, formation of the SBL delay by 3-4 hours after the sunset. Thus, we cannot expect a perfect diurnal variation in all the cases, especially when the SBL formation is delayed. In order to study the diurnal variation of the ABL, we have segregated all the CBL and SBL observed at 3-h intervals during the diurnal cycle in different seasons. Similarly, all the cases of the CBL and RL observed at 3-h intervals are averaged into different seasons.

Figures 10a-10b show the diurnal variation of the ABL_{CS} and ABL_{CR} during different seasons. In general, the CBL heights vary between 1.05±0.46 km to 2.25±0.72 km, the SBL heights vary between 0.15±0.05km to 0.33±0.27kmand the RL heights varyfrom1.39±0.41 km to 1.94±0.63 km. We have also obtained the diurnal variation of the surface temperature during different seasons as shown in Fig 10c. In general, the diurnal patterns of the ABL_{CS} and ABL_{CR} during different seasons are same as annual mean pattern shown in Fig 9a and Fig 9b, respectively. The diurnal variation of the ABL_{CS} shows a seasonal pattern such that CBL attain maximum height during the summer monsoon while the SBL during the winter to pre-monsoon. The amplitude of the diurnal evolution of the ABL_{CS} is stronger during pre-monsoon when compared to other seasons, i.e. maximum to minimum height variation is more during pre-monsoon when compared to other seasons. The SBL attains maximum height at 0200 IST. Fig 10b shows that the ABL_{CR} height has a weak diurnal pattern during the winter when compared to summer. It is interesting to note that the CBL and RL heights reverse their seasonal pattern. The CBL height is higher during the summer and is lower during the winter in contrast, to the RL height, which becomes higher during the winter and lower during the summer. In general, the CBL attains maximum height at 1400-1700 IST and minimum during 0800-1100 IST during all seasons.

Figure 10c and 10d show the diurnal variation of the surface temperature and LCL during different seasons, respectively. Both the surface temperature and the LCL are the highest and lowest during pre-monsoon and winter, respectively. The highest amplitude of the diurnal variation of the ABL_{CR} can be attributed to the highest surface temperature during pre-monsoon. Similarly, the weak diurnal pattern of the ABL_{CR} can be attributed to the lowest surface temperature during the winter. In general, the LCL is lower than ABL_{CR} throughout the year. The difference between the LCL and CBL height is more during the winter and post-monsoon than pre-monsoon and summer monsoon.

As mentioned earlier, the diurnal evolution of the annual and seasonal mean pattern of the ABL is closely associated with the surface temperature. In order to see their 3-hourly relationships, we obtained the scatter plot of the CBL, RL and SBL with the surface temperature as shown in Figs. 11a-c, respectively. Broadly, the scatter diagram indicates that warmer is the surface, the higher is the CBL and RL and vice versa (Figs. 11a-b). However, these features are not always consistent and several times they occur randomly. In contrast to the CBL and RL, SBL higher is higher over the colder surface and vice versa, however, these features also are not always consistent and several times they occur randomly (Fig. 11c). The corresponding 3-hourly relationship between the LCL and CBL, RL and SBL are shown in Figs 11d-c, respectively. The scatter plot between the CBL and LCL indicate that they occur randomly. The LCL generally occurs either below or at the CBL and RL except a

Deleted: ¶
Deleted: 9
Deleted: 9a
Deleted: 9b
Deleted: 9c
Deleted: 8a
Deleted: 8b
Deleted: 9b
Deleted: 9c
Deleted: s
Deleted: ;
Deleted: is

few times when it occurs above the CBL and RL (Figs. 11d-e). The cases when the LCL occurs above the CBL or RL, clouds may not be generated by the processes driven by the ABL and can be formed due to large scale-dynamics (Anurose et al., 2016). We observed no relationship between the SBL and LCL (Fig. 11f). For the SBL case, as the vertical motion is inhibited, the relationship between the LCL and SBL is irrelevant (Anurose et al., 2016). Anurose et al., (2016) also studied the relationship between the CBL height and the LCL over the coastal station, Thiruvananthapuram (8.5◦ N, 76.9◦ E), they did not observed any relationship. However, the LCL over Thiruvananthapuram is found to higher than ABL for a majority of the database in contrast to Gadanki.

Figures 12a and 12b show the schematic representation of the diurnal evolution of the mean ABL from 11:00 IST on the first day to 11:00 IST on the second day during the winter and summer monsoon seasons, respectively. The diagram is generated from the seasonal mean ABL height data presented in Figs.10a and 10b. The vertical cross section of the ABL characterizing the seasonal mean CBL, SBL, RL, and entrainment zone (E.Z.), capping inversion and the LCL obtained from the observed data over Gadanki. The schematic diagram represents the typical evolution of the boundary layer, consistent to the diagram presented in the Stull (1988) and Wallace and Hobbs (2006). The CBL during the winter evolves slowly when compared to summer monsoon season in which the ABL growth is rapid. The SBL starts to form well before the sunset during both seasons; however, it remains persistent, even after the sunrise only during the winter season. During the winter, the RL remains almost constant throughout the night. However, during the summer, the RL rapidly decreases as the night passes. The capping inversion during the summer is thicker when compared to the summer monsoon. We have also shown the seasonal mean LCL which occurs within the CBL and RL during both seasons. Note that the transition regions (from the CBL to RL during evening transition and the RL to CBL during morning transition) cannot be accurately represented with available time resolutions. Thus, the part of the CBL after the sunset and the part of the RL after the sunrise may not possess any meaning. This schematic diagram clearly represents the typical (Fig.4), annual mean (Fig.9) and seasonal mean (Fig.10) characteristic of the ABL.

3.7 Qualitative relationships between cloud top height (CTH) and ABL_{CR} height

The presence of the clouds has a large impact on the boundary layer structure. However, it leads to considerable complication because of the important role played by radiative fluxes and phase change (Garratt, 1992). The relationship between the CTH and the CBL/RL is obtained and is shown in Fig. 13. We have observed the CTH at various layers ranging from within the ABL to up to 12 km during the different campaigns. The CTH relative to the ABL_{CR} is obtained for each individual campaign, which is listed in Table1. In total, for 630 cases the clouds were present either below or near to or above the ABL_{CR}. Rest of 50 cases are when the clear sky conditions observed. Note that in total 680 cases, when CBL and RL are defined. We observed that in total 175, 199, 222 and 34 cases, when CTH occurred within ± 0.5 km, below 0.5 km, above 0.5 km but below 6.0 km, and above 6.0 km of the ABL_{CR}, respectively. These cut off heights regions are selected through visual inspection by trial and error after examining several ABL height and CTH timeseries. The timeseries of the CTH, ABL_{CR} and LCL for the cases when the CTH occurred within ± 0.5 km, below 0.5 km, above 0.5 km but below 6.0 km of ABL_{CR} are shown in Fig 13. The CTH within ± 0.5 km of the ABL_{CR} is positively correlated (r = 0.88) with SD of 0.28 km (Fig 13a). Fig 13a further reveals a clear association between the ABL_{CR} and the CTH variations. These cases indicate the cloud topped boundary layer (CTBL) where clouds are limited in their

Formatted: Font color: Text 1

Deleted: ¶
¶

Deleted: 10

Deleted: and

Deleted:

Deleted: 10

Deleted: 10a

Deleted: 10a

vertical extent by main capping or subsidence inversion (Garratt, 1992). Fig. 13b shows that the CTH occurring below 0.5 km of the ABL_{CR} is also positively correlated (r = 0.71) with SD of 0.37 km. Although these clouds occur well below the ABL_{CR}, both vary in the similar fashion (Fig 13b). It can be seen that higher the cloud level higher the ABL_{CR} and vice versa. Similarly, the ABL_{CR} height variation is also well correlated (r = 0.58) with the CTH variation occurring above 0.5 km but below 6.0 km of the ABL_{CR} (Fig 13c).

When the CTH is within ± 0.5 km of the ABL_{CR}, LCL occurs mostly below the ABL, except a few cases when it coincides with either the ABL or CTH (Fig.13a). When the CTH is below 0.5 km of the ABL_{CR} the LCL again occurs mostly below the ABL but generally coincided with the CTH (Fig.13b). In this case, the LCL sometimes also occurs above the CTH. The clouds occurring below the ABL could be the shallow clouds, in such cases LCL representing the cloud base may occur near to the CTH. However, it is to be noted that the CTH represents the cloud condition for the area averaged over 0.25° latitude X 0.25° longitude regions, whereas the LCL indicates the cloud base exactly over the observation site. Thus, the LCL may not always agree with the CTH when the cloud is not extended over the larger area. For the cases when the clouds occurring above 0.5 km but below 6.0 km of the ABL_{CR}, the LCL mostly occurs either below the ABL or generally coincides with the ABL (Fig 13c).

It is interesting to note that when the CTH is below the ABL_{CR}, CBL and RL occur at higher height (mostly above 2 km) whereas when the CTH is above the ABL_{CR}, CBL and RL occur at a lower height (mostly below 2.0 km). Generally, the CBL (sometimes also called as fair weather boundary layer) occurs at lower height during a shallow cumulus when compared to clear sky conditions (Medeiros et al., 2005). Very deep convective clouds do not show any relationship with the ABL_{CR} variation (figure not shown) as can be seen from Fig. 4b. Qualitatively, it indicates that the presence of the clouds near to the CBL and RL directly impact its variation, but not the high level clouds due to the deep convection events. It is to be noted that there are two occasions when rainfall occurred during the campaign periods, however, these few data do not reveal any relation between the ABL and rainfall.

4 Discussion and Conclusions

The unique and long term intensive campaigns of high vertical resolution radiosonde observations on multiple of 3 hours over a tropical location, Gadanki, in the Indian monsoon region reveal the clear diurnal structure of the ABL height. The high vertical resolution of the radiosonde data enables us to detect the SBL height directly, which otherwise was very difficult.

Identification of the ABL is generally preferred using θ_v and q obtained from radiosonde observation because they can represent the mixing height better than the T. However, we observed an excellent correlation between T and θ_v suggesting that ABL can be identified using T. Moreover, use of T can give both elevated inversion as well as surface based inversion well suited to study the diurnal variation of the ABL. The limitation of using T is that it can also identify mid-level inversions sometimes. However, to avoid mid-level inversions, if any, we have restricted the ABL height identification below 3.5 km. In case of multiple inversions, the lower one having 80% of main inversion is considered. The correlation between T (or θ_v) and N are in good agreement with Basha and Ratnam, (2009). We also found that N yields the ABL height lower than that of T several times, but not always, in contrast to Chennai located 120 km southeast of Gadanki where significant ABL height difference of ~ 0.84 (between θ and N) is observed in evening soundings (Seidel et al., 2010).

Deleted: 10b

Deleted: 10b

Deleted: 10c

Formatted: Subscript

Deleted: ¶

Deleted:

The nighttime ABL is complex to define when compared to daytime ABL. As the nighttime ABL or the SBL depends on the surface cooling, if it delays, or does not form at all, which generally happens, one will find it as about same as pervious daytime ABL (i.e CBL). It is the part of the daytime mean state and has not formed due to action of nightime surface forcing. However, as it is above the surface, which is an only criterion left to assign the RL as the ABL in the absence of the SBL(Liu and Liang, 2010). But, if the measuring instrument has limited capability to detect the SBL, one will land in defining the RL as nighttime ABL, which will not be at rue representation of the ABL height.

Deleted: the nighttime ABL

In total, the SBL forms about 50% times during the midnight to morning. In the early part of the night, the SBL occurs less frequently (33%) than late night and hence indicates the delay in the surface cooling process. The SBL forms more frequently during winter season when compared to other seasons. Thus, diurnal variation of the ABL occurs more often during winter than the summer. There could be various reasons for the delay in the SBL formation, such as cloud cover or wet surface due to rain which can disturb or delay the surface cooling process. Sandeep et al, (2015) observed that the ABL over Gadanki after the sunset becomes shallower and its growth delayed by 1–4 h during wet episodes. Over Indian region, clouds and precipitation most frequently occur during the summer monsoon season when compared to the winter season, suggesting the formation of the SBL will be less frequent during the former season consistent to the observed result. However, irrespective of the season the surface temperature shows a diurnal pattern. Thus, another possibility of less occurrence of the SBL during summer monsoon season could be due to high night time temperature. In fact the nighttime surface temperature during summer monsoon as well as post and pre monsoons are greater than that of daytime surface temperature during the winter season. Though, the surface temperature during these seasons decreases during nighttime, it doesn't have sufficient cooling effect as winter season probably preventing the formation of the SBL most of the time during the summer season. Thus, it could be possible that even though the surface temperatures show diurnal variation during the summer monsoon, diurnal variability in the ABL may not be expected.

The minimum height of the CBL at 0800 IST is due to weak convection (thermals) during the morning hours when compared to other timings of the day. As convection becomes stronger (the strongest surface warming at 1400 IST) due to the strong thermals, the CBL becomes higher and reaches a maximum height at 1400-1700 IST. Similarly, as the night passes, surface cooling becomes stronger (the strongest cooling occurs at 0200 IST) leading to higher SBL height at 0200 IST -0500 IST. The RL remains sometimes at similar height as the CBL in case of very strong gradient in moisture and temperature. But generally it lowers down as time passes during the night, especially during the summer monsoon season. As daytime convection is switched off during the night, the turbulence strength goes weaker and weaker as night passes leading to decrease in the RL height.

During the pre-monsoon, the surface temperature has the strongest diurnal variation which manifests stronger diurnal variation of the ABL_{CR} height (Angevine et al., 2001). But higher CBL occurs during the summer monsoon season and not during the pre-monsoon. The higher CBL during summer monsoon season is due to stronger convection occurring in this season when compared to the other seasons. During the winter season, the surface temperature is low leading to a weak diurnal pattern of the ABL_{CR} (Angevine et al., 2001). Since convection is weaker during the winter season, the CBL is at a lower height when compared to the other seasons. The reversal of the CBL and RL height patterns between summer monsoon and winter is due to the surface temperature variation and strength of convection. It is due to the fact that during the winter the RL does

not lower as observed for the other seasons due to less surface temperatures, while the CBL becomes higher during summer monsoon seasons due to stronger convection when compare to the winter. Thus, the CBL is lower during the winter, but it is higher during summer monsoon while RL is higher during the winter but it is lower during the summer monsoon season.

Finally, the qualitative relationship between the ABL_{CR} height, the CTH and the LCL is examined. We only provide here qualitative information based on the CTH obtained using merged TBB data, since direct observation of the CTH over the launch site during the campaign periods are not available. As observed in this study, the CTH at various layers has been observed using ceilometer at Ahmedabad (23.03◦ N, 72.54◦ E), India (Sharma et al., 2016). As suggested by Wang and Rassow (1995), the various cloud layers can be obtained utilizing the RH data (Wang and Rassow, 1995). However, as the criteria for fixing the cloud base and top heights using the RH data has not been finalized for the tropical clouds occurring over this region, we have preferred satellite derived CTH data in this study. We also obtained the LCL height, but for majority of the database LCL occurs below the ABL and they are randomly related consistent to Anurose et al., (2016). Thus, we have interpreted our results based on the CTH data only. If the clouds occur above the ABL_{CR} during the daytime, they will absorb the incoming solar radiation and hence cool the surface. This in turn will weaken the thermals and hence decrease the CBL height. On the other hand, when the clouds occur below the CBL, it will cool the surface, but warm the region between cloud top and CBL and hence can strengthen the thermals which will lead to increase the CBL height. This explains why CBL is at lower height when the clouds above it and at the higher height when clouds below it. If the cloud occurs during nighttime, the situation will be more complex and difficult to explain the RL variability. During nighttime, the clouds will block the outgoing long wave radiation, which in general warm below the RL and hence disturb the surface cooling and the formation of the SBL. The verification of the CTH height using space borne satellites and ground based observations such as ceilometer over the launch site will be carried out as a separate study in the future.

Following are the main findings on the diurnal variability of the atmospheric boundary layer (ABL):

1. The convective boundary layer (CBL) height has a large variation ranging from as low as 0.4 km to as high as about 3.0 km above the surface and occurs uniformly at 3-h intervals during the diurnal cycle over Gadanki, a tropical station in the Indian monsoon region.
2. The stable boundary layer (SBL) mainly forms during night time; however, it can also form during daytime, especially during evening and morning hours, i.e. during transition periods. The SBL forms about 50% of times of total observations during 2300-0500 IST. At 2000 IST, occurrence of the SBL is only 33%, indicating that delay in surface cooling for about 17% of the times. About 25 % of the time the SBL forms at 0800 IST indicating the dominance of the surface cooling even after the sunrise. As surface cooling starts well before the sunset, sometimes the SBL (about 9%) also forms at 1700 IST.
3. The overall mean SBL lies well within the 0.3 km and the mean CBL lies well within 3.0 km consistent with the available literature. However, the maximum probability distribution of the SBL occurs at 0.15 km lower than its mean value. In contrast to the SBL, the maximum probability distribution of the CBL coincides with mean CBL at about 2 km for the winter season and the whole year. The maximum

Deleted: and

Formatted: Font color: Auto

Formatted: Font color: Auto

Formatted: Font color: Auto

Formatted: Font color: Text 1

Deleted:

Deleted: the

probability distribution of the CBL during the summer monsoon season has a broader peak when compare to winter season.

4. The CBL and the RL heights obtained using different methods (T, θ_v, q and N) correlates well.
5. A clear diurnal variation of the ABL_{CS} height over the different seasons is observed with the maximum CBL height during the summer monsoon season while the maximum SBL height during the winter to pre-monsoon. The seasonal pattern reverses for the RL height that becomes higher during the winter and lower during the summer monsoon season.
6. The ABL_{CR} height is positively correlated with the CTH occurring near to it, however, the deep convective clouds do not show any relationship. When the cloud is at lower height the ABL_{CR} is relatively higher and vice versa. This needs to be verified using independent observations of the CTH perhaps using Ceilometer observations.
7. Over Gadanki, the LCL occurs below the CBL and RL for the majority of the database and they are randomly related.

Acknowledgements. We thank NARL radiosonde operation team for conducting the experiment under tropical tropopause dynamics (TTD) campaigns fully supported by the Indian Space Research Organization as a part of CAWSES India Phase-II program.

References

Angevine, W. M., Baltink, H. K., and Bosveld, F. C.: Observations of the morning transition of the convective boundary layer, Bound.-Lay. Meteorol., 101, 209-227, 2001.

Anurose, T.J., Subrahamanyam, D.B. and Sunilkumar, S.V.: Two years observations on the diurnal evolution of coastal atmospheric boundary layer features over Thiruvananthapuram (8.5◦ N, 76.9◦ E), India. Theoretical and Applied Climatology, pp.1-14, 2016.

Ao, C. O., Waliser, D. E., Chan, S. K., Li, J. L., Tian, B., Xie, F., and Mannucci, A. J.: Planetary boundary layer heights from GPS radio occultation refractivity and humidity profiles, J Geophys Res.-Atmos., 117, 2012.

Basha, G. and Ratnam, M. V.: Identification of atmospheric boundary layer height over a tropical station using high-resolution radiosonde refractivity profiles: Comparison with GPS radio occultation measurements, J Geophys Res.-Atmos., 114, 2009.

Bianco, L., Djalalova, I., King, C., and Wilczak, J.: Diurnal evolution and annual variability of boundary-layer height and its correlation to other meteorological variables in California's Central Valley, Bound.-Lay. Meteorol., 140, 491-511, 2011.

Bolton D.: The computation of equivalent potential temperature, Mon. Weather Rev., 108,1046–1053, 1980.

Brill, K. and Albrecht, B.: Diurnal variation of the trade-wind boundary layer. Mon. Weather Rev., *110*(6), pp.601-613,1982.

Chan, K. M. and Wood, R.: The seasonal cycle of planetary boundary layer depth determined using COSMIC radio occultation data, J Geophys Res.-Atmos., 118, 2013.

Chandrasekhar Sarma, T., Narayana Rao, D., Furumoto, J., and Tsuda, T.: Development of radio acoustic sounding system (RASS) with Gadanki MST radar–first results, 2008, 2531-2542.

Clifford, S. F., CHANDRAN KAIMAL, J., Lataitis, R. J., and Strauch, R. G.: Ground-based remote profiling in atmospheric studies: An overview, Proc. IEEE, 82, 313-355, 1994.

Deardorff, J. W.: Parameterization of the planetary boundary layer for use in general circulation models 1, Mon. Weather Rev., 100, 93-106, 1972.

Garratt, J.: The atmospheric boundary layer, Cambridge atmospheric and space science series, Cambridge University Press, Cambridge, 416, 444, 1992.

Garratt, J. R.: Review: the atmospheric boundary layer, Earth-Sci. Rev., 37, 89-134, 1994.

Hashiguchi, H., Yamanaka, M.D., Tsuda, T., Yamamoto, M., Nakamura, T., Adachi, T., Fukao, S., Sato, T. and Tobing, D.L.: Diurnal variations of the planetary boundary layer observed with anL-band clear-air doppler radar. Boundary-Layer Meteorology, 74(4), pp.419-424,1995a.

Hashiguchi, H., Fukao, S., Tsuda, T., Yamanaka, M.D., Tobing, D.L., Sribimawati, T., Harijono, S.W.B. and Wiryosumarto, H.: Observations of the planetary boundary layer over equatorial Indonesia with an L band clear-air Doppler radar: Initial results. Radio Science, 30(4), pp.1043-1054,1995b.

Holtslag, A. and Nieuwstadt, F.: Scaling the atmospheric boundary layer, Bound.-Lay. Meteorol., 36, 201-209, 1986.

Konor, C. S., Boezio, G. C., Mechoso, C. R., and Arakawa, A.: Parameterization of PBL processes in an atmospheric general circulation model: description and preliminary assessment, Mon. Weather Rev., 137, 1061-1082, 2009.

Formatted: Font: (Asian) +Body Asian (MS Mincho), (Asian) Japanese

Deleted: ¶

Formatted: Font: (Asian) +Body Asian (MS Mincho), (Asian) Japanese

Formatted: Font: Not Italic

Formatted: Font: Not Italic

Formatted: Font: Not Italic

Formatted: Font: Not Italic

Formatted: Font: (Asian) +Body Asian (MS Mincho), (Asian) Japanese

Kumar, K. K. and Jain, A.: L band wind profiler observations of convective boundary layer over Gadanki, India (13.5 N, 79.2 E), Radio Sci., 41, 2006.
Kumar, M. S., Anandan, V., Rao, T. N., and Reddy, P. N.: A climatological study of the nocturnal boundary layer over a complex-terrain station, J. Appl. Meteorol. Clim., 51, 813-825, 2012.
Liu, S. and Liang, X.-Z.: Observed diurnal cycle climatology of planetary boundary layer height, J. Climate, 23, 5790-5809, 2010.
May, P.T., Long, C.N. and Protat, A.:. The diurnal cycle of the boundary layer, convection, clouds, and surface radiation in a coastal monsoon environment (Darwin, Australia). Journal of Climate, 25(15), pp.5309-5326,2012.
Medeiros, B., Hall, A., and Stevens, B.: What controls the mean depth of the PBL?, J. Climate, 18, 3157-3172, 2005.
Mehta, S. K., Ratnam, M. V., and Krishna Murthy, B.: Multiple tropopauses in the tropics: A cold point approach, J Geophys Res.-Atmos., 116, 2011.
Ratnam, M. V., Sunilkumar, S., Parameswaran, K., Murthy, B. K., Ramkumar, G., Rajeev, K., Basha, G., Babu, S. R., Muhsin, M., and Mishra, M. K.: Tropical tropopause dynamics (TTD) campaigns over Indian region: An overview, J. Atmos. Sol-Terr. Phy., 121, 229-239, 2014.
Sandeep, A., Rao, T. N., and Rao, S.: A comprehensive investigation on afternoon transition of the atmospheric boundary layer over a tropical rural site, Atmos. Chem. Phys., 15, 7605-7617, 2015.
Santanello Jr, J.A., Friedl, M.A. and Ek, M.B.: Convective planetary boundary layer interactions with the land surface at diurnal time scales: Diagnostics and feedbacks. Journal of Hydrometeorology, 8(5), pp.1082-1097, 2007.
Schmid P. and Niyogi D: A Method for Estimating Planetary Boundary Layer Heights and Its Application over the ARM Southern Great Plains Site, J.Atmos. Ocean. Tech., 29,316-322, 2012.
Seibert, P., Beyrich, F., Gryning, S.-E., Joffre, S., Rasmussen, A., and Tercier, P.: Review and intercomparison of operational methods for the determination of the mixing height, Atmos. Environ., 34, 1001-1027, 2000.
Seidel, D. J., Ao, C. O., and Li, K.: Estimating climatological planetary boundary layer heights from radiosonde observations: Comparison of methods and uncertainty analysis, J Geophys Res.-Atmos., 115, 2010.
Seidel, D. J., Zhang, Y., Beljaars, A., Golaz, J. C., Jacobson, A. R., & Medeiros, B.: Climatology of the planetary boundary layer over the continental United States and Europe, J Geophys Res.-Atmos., 117, 2012.
Sharma, S., Vaishnav, R., Shukla, M. V., Kumar, P., Kumar, P., Thapliyal, P. K., Lal, S., and Acharya, Y. B.: Evaluation of cloud base height measurements from Ceilometer CL31 and MODIS satellite over Ahmedabad, India, Atmos. Meas. Tech., 9, 711-719, 2016.
Shravan Kumar, M. and Anandan, V.: Comparision of the NCEP/NCAR Reanalysis II winds with those observed over a complex terrain in lower atmospheric boundary layer, Geophys. Res. Lett., 36, 2009.
Sokolovskiy, S., Kuo, Y. H., Rocken, C., Schreiner, W., Hunt, D., and Anthes, R.: Monitoring the atmospheric boundary layer by GPS radio occultation signals recorded in the open-loop mode, Geophys. Res. Lett., 33, 2006.
Stull, R. B.: An introduction to boundary layer meteorology, Atmospheric Sciences Library, Dordrecht: Kluwer, 1988, 1, 1988.
Tucker, S. C., Senff, C. J., Weickmann, A. M., Brewer, W. A., Banta, R. M., Sandberg, S. P., Law, D. C., and Hardesty, R. M.: Doppler lidar estimation of mixing height using turbulence, shear, and aerosol profiles, J.Atmos. Ocean. Tech., 26, 673-688, 2009.
Van Den Broeke, M.R.: Structure and diurnal variation of the atmospheric boundary layer over a mid-latitude glacier in summer. Boundary-Layer Meteorology, 83(2), pp.183-205, 1997.
van der Kamp, D. and McKendry, I.: Diurnal and seasonal trends in convective mixed-layer heights estimated from two years of continuous ceilometer observations in Vancouver, BC, Bound.-Lay. Meteorol., 137, 459-475, 2010.
Wallace J.M., Hobbs, P.V.: Atmospheric science an introductory survey, second edition. International Geophysics series, Acadamic Press 92, 483 pp, 2006.
Wang, J. and Rossow, W.B.: Determination of cloud vertical structure from upper-air observations. Journal of Applied Meteorology, 34(10), pp.2243-2258, 1995.

Formatted: Font: (Asian) +Body Asian (MS Mincho), (Asian) Japanese

Formatted: Font: (Asian) +Body Asian (MS Mincho), (Asian) Japanese

Deleted: ¶

Formatted: Font: (Asian) +Body Asian (MS Mincho), (Asian) Japanese

Formatted: Font: Not Italic

Formatted: Font: Not Italic

Formatted: Font: (Asian) +Body Asian (MS Mincho), (Asian) Japanese

Formatted: Font: (Asian) +Body Asian (MS Mincho), (Asian) Japanese

Table 1: List of 3-days campaigns conducted during the period December 2010-March 2014. Total number of observations, rejection of bad quality data, the SBL, the CBL and the RL are listed for each campaign. Shaded regions with italic fonts indicate campaigns with more than 90% of the SBL defined. Bold indicates those campaigns where SBL is not defined and the rest when the SBL occur intermittently. CTH relative to ABL are also listed.

SN	Period	No of Observations					
		Total	Rejected	SBL	CBL	RL	CTH-ABL
1	*28 Dec 2010-31 Dec 2010*	*24*	*0*	*10*	*12*	*12*	*±1.5*
2	*17 Jan 2011-20 Jan 2011*	*24*	*0*	*14*	*10*	*6*	*-2.0-1.0*
3	*08 Feb 2011-11 Feb 2011*	*24*	*0*	*14*	*11*	*7*	*-2.0-1.0*
4	**26 Apr 2011-29 Apr 2011**	**24**	**2**	**0**	**11**	**10**	**-1.0-2.0**
5	18 May 2011-21 May 2011	24	1	5	8	9	-1.0-7.0
6	**20 Jun 2011-23 Jun2011**	**24**	**0**	**0**	**12**	**12**	**-1.5-1.0**
7	**21 Jul 2011-24 Jul 2011**	**24**	**0**	**0**	**12**	**12**	**-1.5-2.0**
8	17 Aug 2011-20 Aug2011	24	1	5	10	9	-1.5-1.0
9	*12 Sep 2011-15 Sep 2011*	*24*	*1*	*11*	*12*	*8*	*±2.0*
10	12 Oct 2011-15 Oct 2011	12	2	6	5	3	±0.5
11	*14 Nov 2011-17 Nov 2011*	*24*	*0*	*13*	*12*	*12*	*-2.0-0.0*
12	08 Dec 2011-11 Dec 2011	23	1	7	11	11	-2.0-8.0
13	18 Jan 2012-21 Jan 2012	17	1	8	7	9	±2.0
14	*23 Feb 2012-26 Feb 2012*	*22*	*0*	*13*	*10*	*11*	*-1.5-2.0*
15	**29 Mar 2012-01 Apr 2012**	**23**	**0**	**0**	**12**	**11**	**-1.0-4.0**
16	01 Apr 2012-04 Apr 2012	24	0	9	11	7	0.5-2.5
17	29 May 2012-01 Jun 2012	23	0	6	12	11	-0.5-1.5
18	26 Jun 2012-29 Jun 2012	23	0	8	10	8	-1.0-2.5
19	24 Jul 2012-27 Jul2012	24	2	4	11	11	-1.5-1.0
20	21 Aug 2012-24 Aug 2012	23	0	8	10	6	-1.5-2.5
21	12 Sep 2012-15 Sep 2012	23	0	7	11	8	-0.5-2.0
22	03 Oct 2012-06 Oct 2012	21	0	6	11	10	±0.5
23	05 Nov 2012-08 Nov2012	12	1	2	6	5	±0.5
24	21 May 2013-24 May 2013	22	1	6	10	10	-1.0-2.5
25	17 Jun 2013-20 Jun 2013	24	0	2	12	12	-1.0-3.5
26	15 Jul 2013-18 Jul 2013	24	0	5	12	12	-1.0-2.0
27	26 Aug 2013-29 Aug 2013	24	0	5	11	7	-1.5-0.5
28	23 Sep 2013-26 Sep 2013	24	0	4	11	6	±1.5
29	28 Oct 2013-31 Oct 2013	21	0	6	11	9	-2.0-5.0
30	**21 Nov 2013-24 Nov 2013**	**19**	**2**	**0**	**8**	**9**	-2.0-5.0
31	*18 Dec 2013-21 Dec 2013*	*24*	*0*	*11*	*12*	*12*	*1.0-11.0*
32	**27 Jan 2014-30 Jan 2014**	**24**	**0**	**0**	**12**	**12**	**-0.5-(-2.0)**
33	**24 Feb 2014-27 Feb 2014**	**24**	**0**	**0**	**12**	**12**	**-2.0-0.5**
34	*25 Mar 2014-28 Mar 2014*	*24*	*1*	*12*	*12*	*11*	*-1.0-7.0*
	Total	764	17	207	360	320	

Deleted: ¶

Formatted: Font: Italic

Formatted: Font: Italic

Formatted: Font: Italic

Formatted: Font: Italic

Formatted: Font: Italic

Formatted: Font: Italic

Formatted: Font: Italic

Formatted: Font: Italic

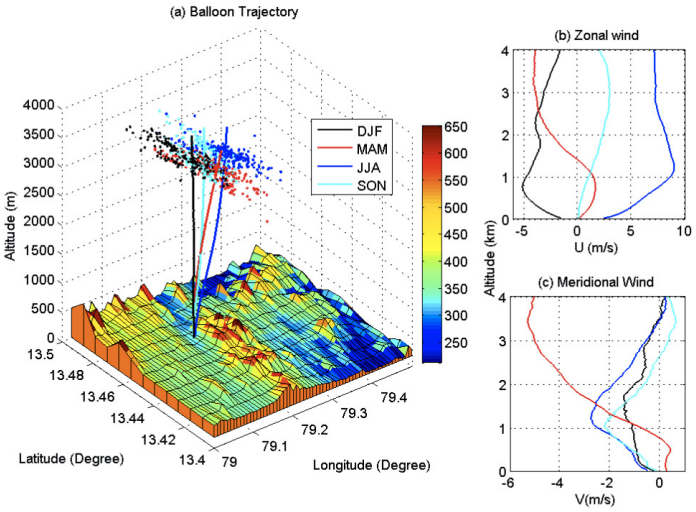

Figure 1: (a) Topographical features surrounding the location of radiosonde launch site, Gadanki (13.45° N, 79.2° E), a tropical station, India, along with profiles of seasonal mean trajectories (thick lines) from the surface to 4 km and the locations of the balloon reaching at altitude 4 km (dots) during different seasons. The mean (b) zonal wind and (c) meridional winds for different seasons observed during the period December 2010-March 2014. Global 30-arc-second gridded topography data is provided by the National Centers for Environmental Information, USA.

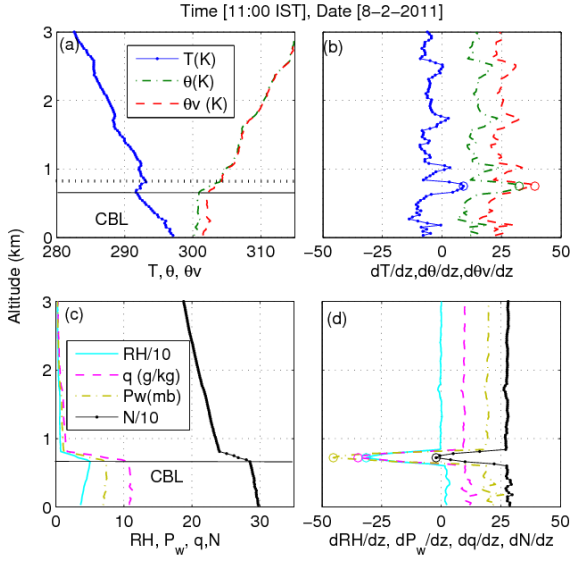

Figure 2:Typical profiles of (a) temperature (T), potential temperature (θ) and virtual potential temperature (θ_v) and (c) relative humidity (RH), specific humidity (q), water vapor pressure (P_w), and radio refractivity (N) showing convective boundary layer (CBL) using GPS radiosonde observation at 1100 IST on February 8, 2011 over Gadanki (13.45°N, 79.2°E). (b) and (d) show the gradient profiles corresponding to (a) and (c), respectively. Solid horizontal lines in (a) and (c) indicates the base of the inversion layer. Dotted line in (a) indicates the top of the inversion. Open circles in figures (b) and (d) denote the CBL heights above ground level.

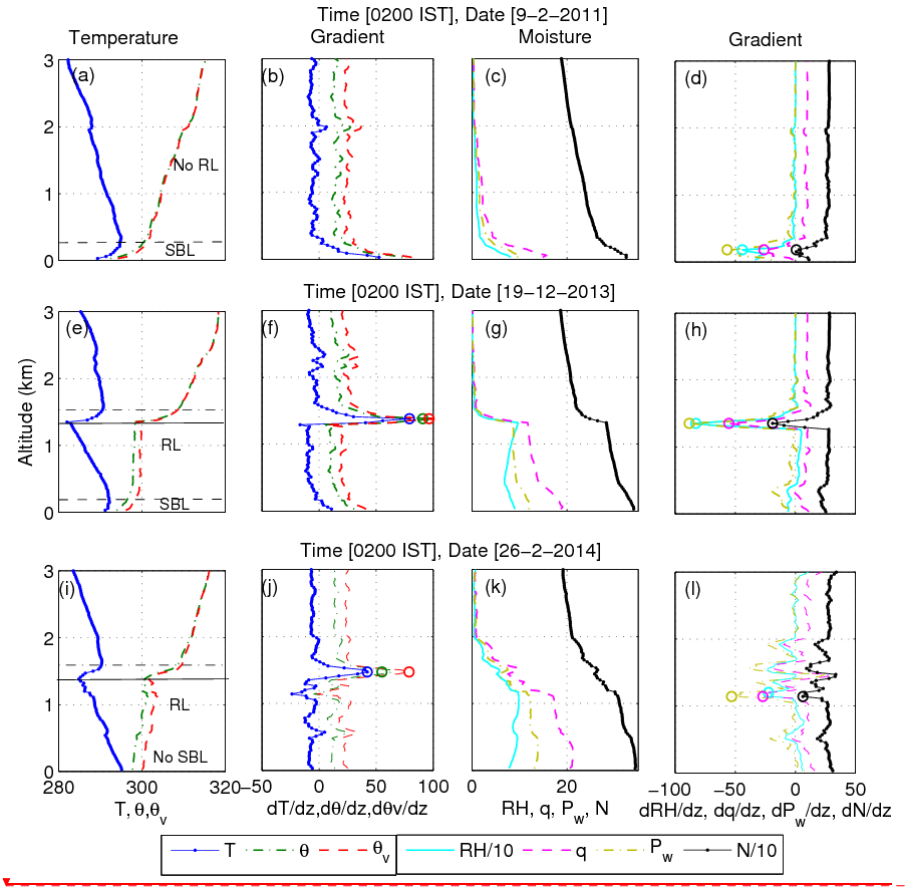

Figure 3: Same as Figure (2) but for night time profiles observed at 0200 IST indicating (a) the stable boundary layer (SBL) only, but not the residual layer (RL) observed on February 9, 2011, (b) both the SBL and the RL observed on December 19, 2013 and (c) the RL but not the SBL observed on February 26, 2014. The horizontal dashed lines denote the surface based inversion in the temperature profile and open circles denote maximum gradients in temperature variables or minimum gradients in the moisture variables. Horizontal dash-dotted lines indicate capping inversion layer.

Deleted: , respectively.

Deleted: on

Deleted: dotted lines

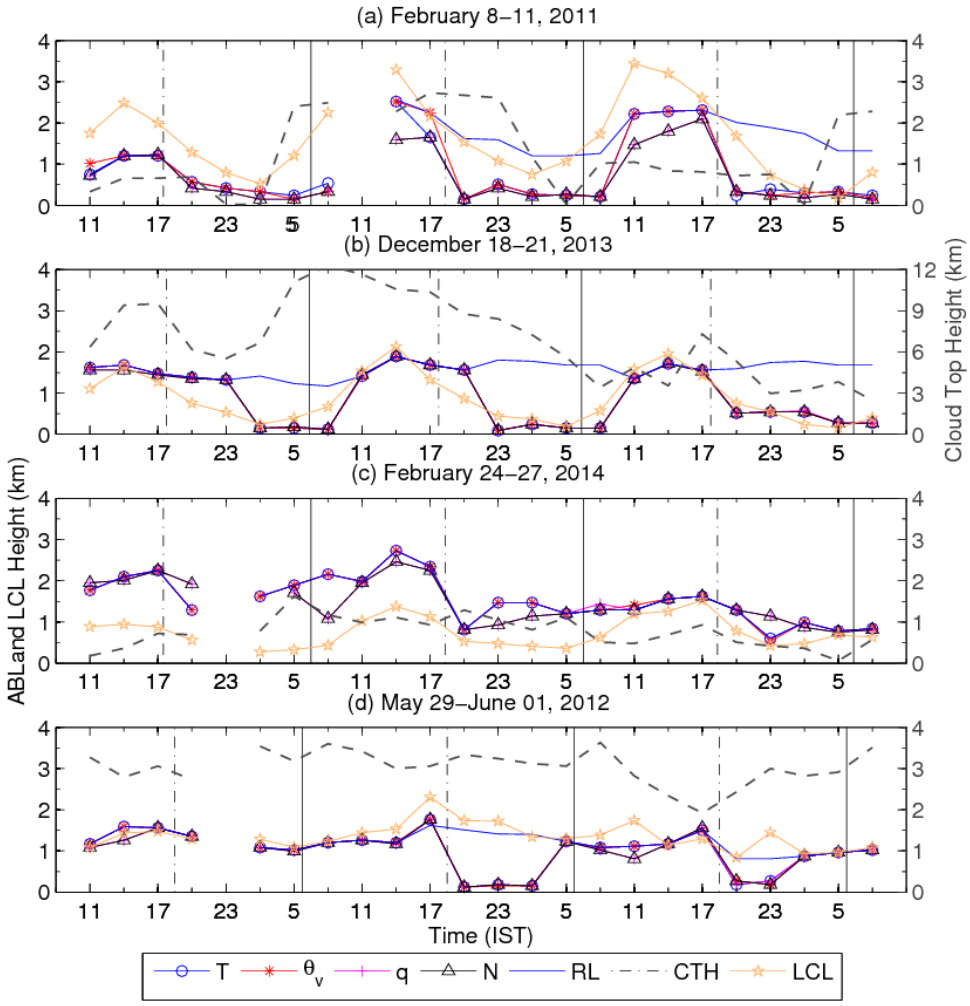

925

Figure 4: Diurnal variability of the ABL (CBL, SBL and RL) height obtained from the variables T, θ_v q, and N during (a) February 8-11, 2011, (b) December 18-21, 2013, (c) February 18-21, 2013, and (d) May 29- June 01, 2012. Thick dashed lines indicate the cloud top height (CTH). Dark yellow star line indicates the lifting condensation level (LCL). Vertical dashed and solid bars indicate sunset and sunrise times, respectively.

930

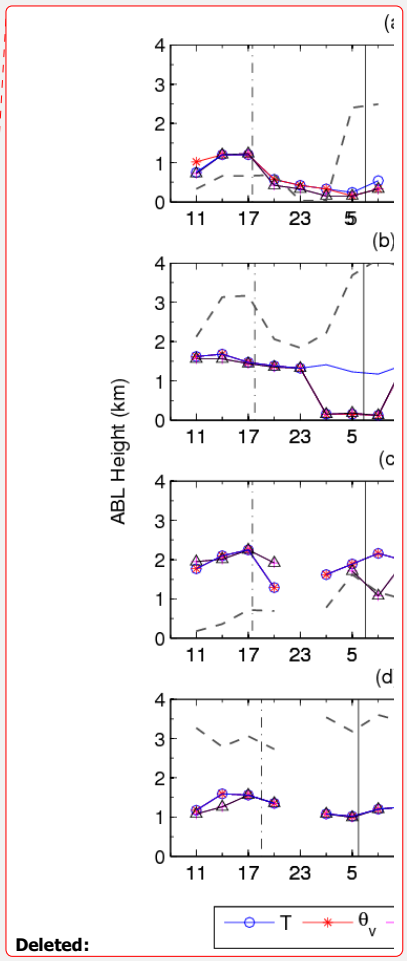

Deleted:

Deleted: rise

Deleted: set

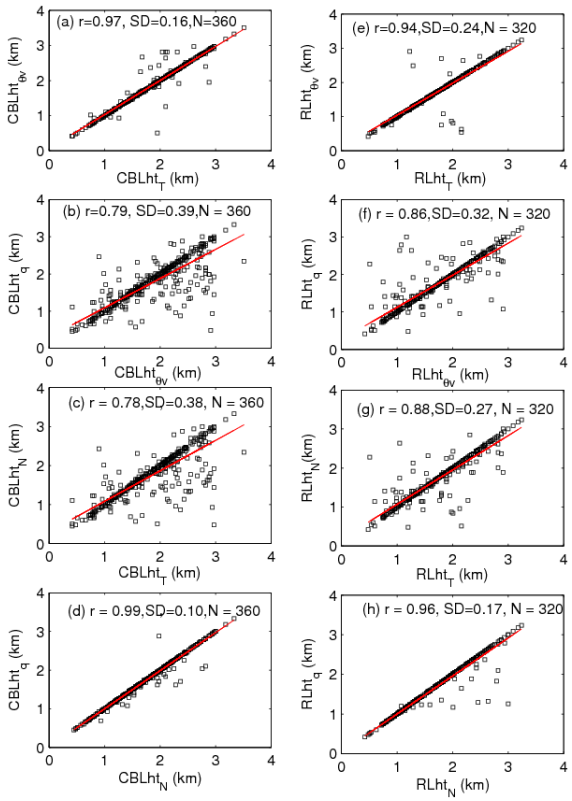

935

Figure 5: (Left panels) Correlation between the CBL heights obtained using (a) *T* and θ_v,(b) $\theta_v$and *q*, (c) *T* and *N*, and(d) *N* and *q*, (Right Panels) (e)-(h) are same as (a)-(d) but the RL heights.

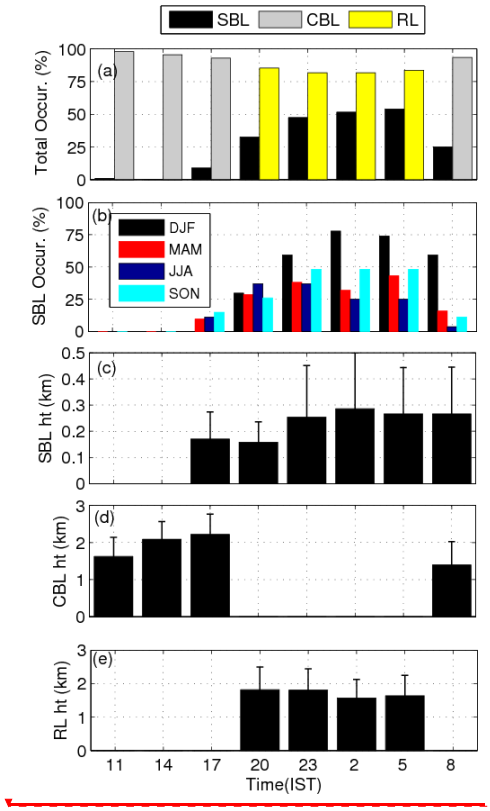

940

Figure 6: (a) Total percentage occurrence of the SBL, CBL, and RL heights (b) percentage occurrence of the SBL during different seasons. Mean and standard deviations of (c) the SBL height observed at 3 hours interval between 1700 IST and 0800 IST, (d) the CBL observed at 3 hours interval between 0800 IST and 1700 IST and (e) the RL observed at 3 hours interval between 2000 IST and 2300 IST. These statistics are obtained using *T* variables.

Deleted:

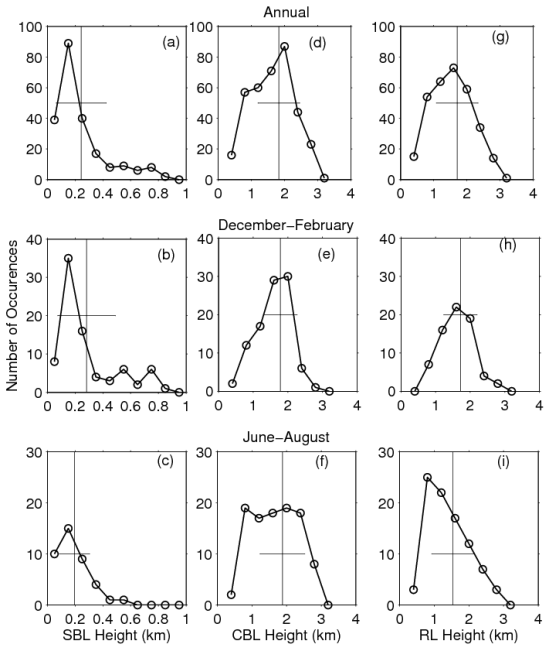

Figure 7: Probability distribution of 3 hourly (left column panels) SBL height with 0.1 km interval obtained for (a) annual (b) winter and (c) summer from the data observed during December 2010-March 2014. (d)-(e) same as (a)-(c) but for the CBL height, and (f)-(h) are same as (a)-(c) but for the RL height with 0.4 km interval. The Points at which the vertical line intersects the x-axis represents their mean heights while the length of the horizontal bar represents the corresponding standard deviations.

Formatted: Normal

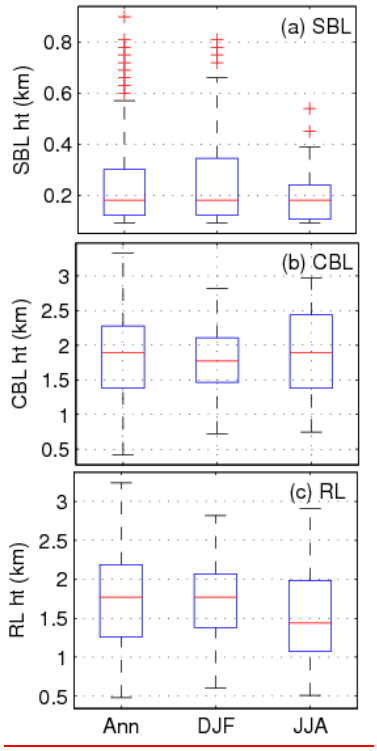

Formatted: Normal, Centered

975 **Figure 8: Boxplot (representing median and interquartile ranges) of (a) SBL height (b) CBL height and (c) RL height for annual (Ann) winter (DJF) and summer monsoon (JJA) from the data observed during December 2010-March 2014.**

Formatted: Font: 9 pt, Bold

Formatted: Normal

Formatted: Font: (Asian) +Body Asian (MS Mincho), (Asian) Japanese

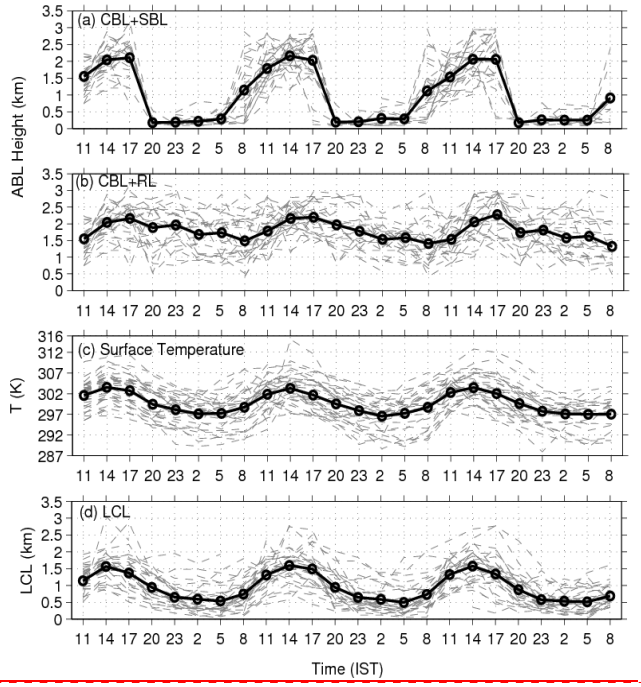

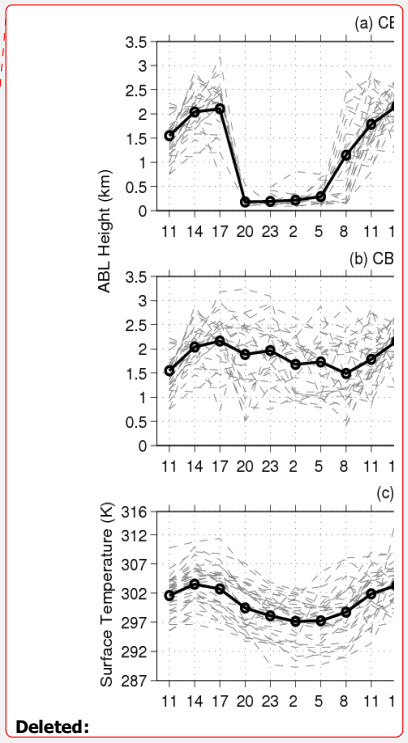

Deleted:

980 **Figure 9: (a) The 3 days diurnal variability of (a) the ABL (CBL+SBL) considering all the data observed for the CBL and SBL, (b) the CBL+RL considering all the data observed for the CBL and RL obtained using *T* variable, (c) the surface temperature, and (d) the LCL height observed during the period December 2010-March 2014.**

Deleted: 8

Deleted: the

Deleted: and

Deleted: S

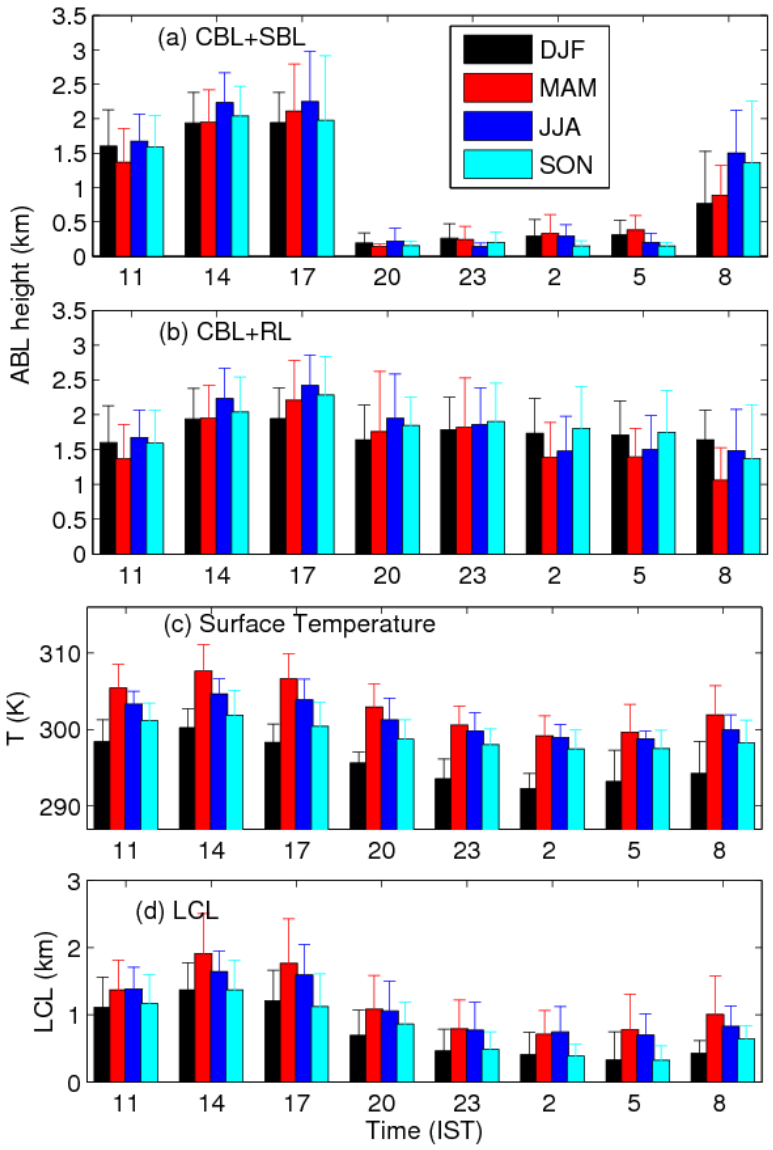

Figure 10: The diurnal variation of (a) the ABL_{CS} (CBL+SBL) height, (b) the ABL_{CR}(CBL+RL) height (c) the surface temperature and (d) the LCL height during different seasons.

Deleted:

Deleted: 9

Deleted: and

Formatted: Normal

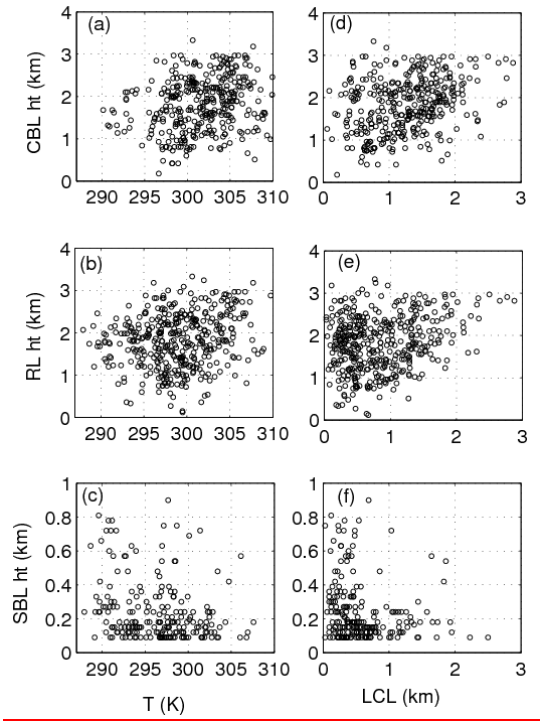

Figure 11: Scatter plot between the surface temperature and (a) CBL, (b) RL, and (c) SBL. (d)-(f) are same as (a)-(c) but for the LCL.

Formatted: Normal, Centered

Formatted: Font: 9 pt, Bold

Formatted: Font: 9 pt, Bold

Formatted: Font: 9 pt, Bold

Formatted: Font: 9 pt, Bold

Formatted: Normal

Formatted: Font: 9 pt, Bold

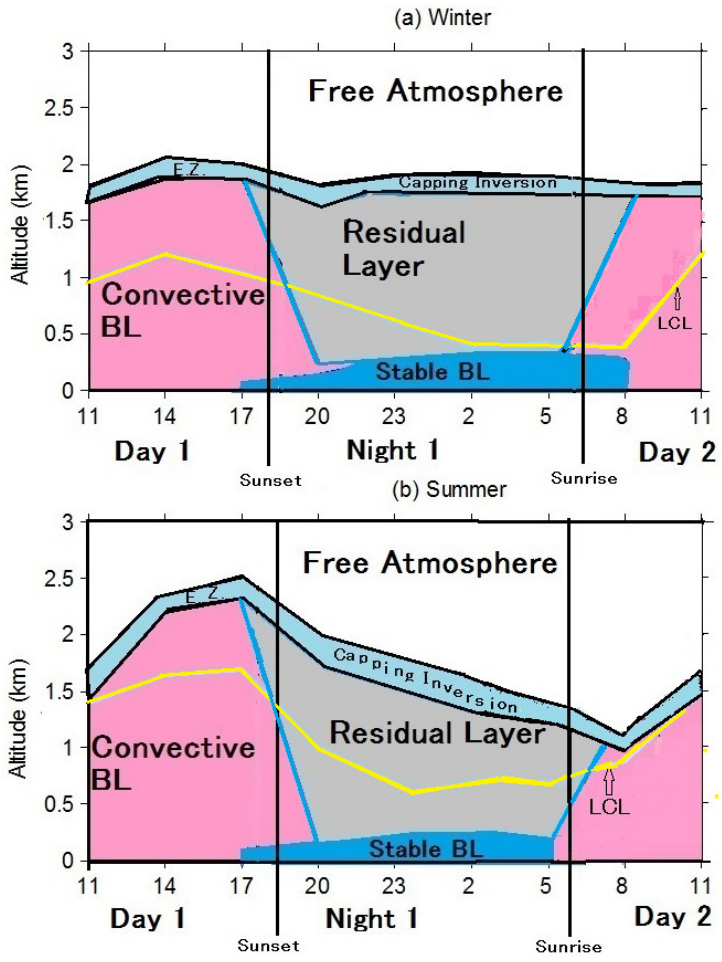

1005

Figure 12: Schematic diagram of the vertical cross section of the mean ABL structure during the (a) winter (DJF) and summer monsoon (JJA) seasons over Gadanki. E.Z. indicates entrainment zone.

Formatted: Normal, Centered

Formatted: Font: 9 pt, Bold

Formatted: Font: 9 pt, Bold

Formatted: Font: 9 pt, Bold

Formatted: Normal

Formatted: Font: 9 pt, Bold

Formatted: Font: (Asian) +Body Asian (MS Mincho), (Asian) Japanese

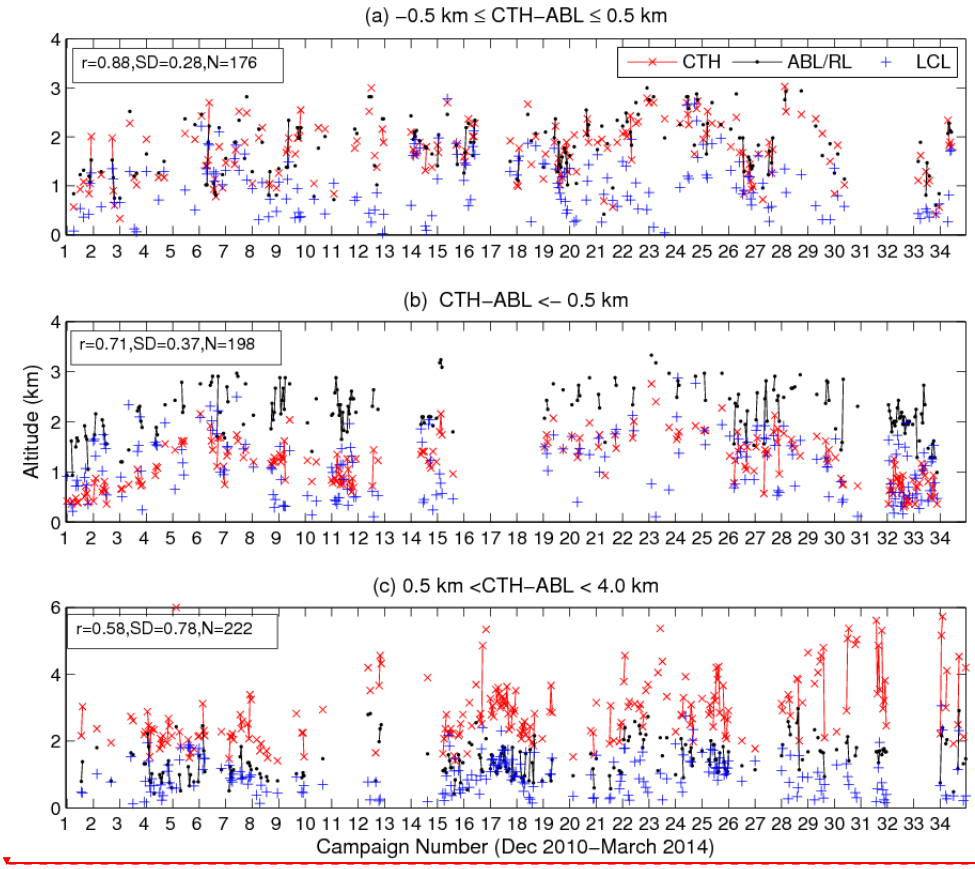

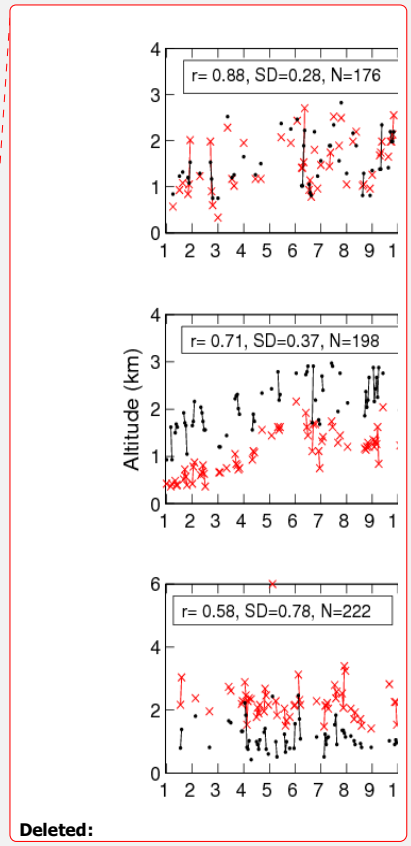

Deleted:

Figure 13:Time series of the CTH, the ABL_{CR} top and the LCL observed for the cases (a) -0.5 km ≤CTH-ABL≤0.5 km (b) CTH-ABL<-0.5 km and (c) 0.5 km <CTH-ABL<4.0 km.

Deleted: 10

Deleted: and